PDGFRα-induced stromal maturation is required to restrain postnatal intestinal epithelial stemness and promote defense mechanisms

Jean-Marie Jacob, Selene Di Carlo, Igor Stzepourginski, Anthony Lepelletier, Papa Diogop Ndiaye, Hugo Varet, Rachel Legendre, Etienne Kornobis, Adam Benabid, Giulia Nigro, et al.

Cell Stem Cell

Article

PDGFRα-induced stromal maturation is required to restrain postnatal intestinal epithelial stemness and promote defense mechanisms

Graphical abstract

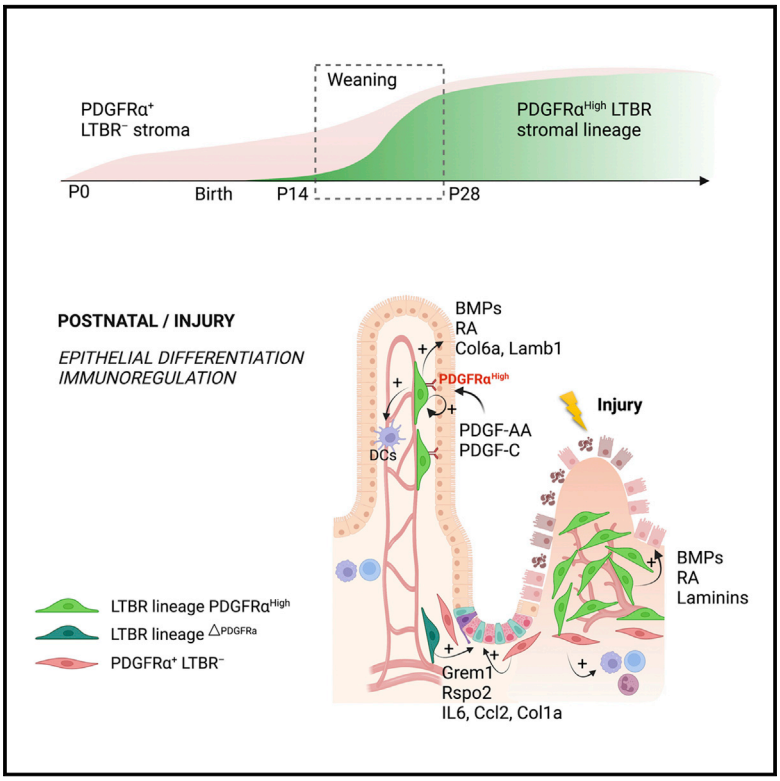

Highlights

- Intestinal LTBR^{+}PDGFRα^{High} stromal lineage develops in the first weeks after birth
- The LTBR stromal lineage restrains stemness and promotes intestinal maturation *in vivo*
- PDGFRα orchestrates spatial and molecular specificities of intestinal stromal niches
- Development of the LTBR lineage is required for postnatal growth and repair responses

Authors

Jean-Marie Jacob, Selene E. Di Carlo, Igor Stzepourginski, ..., Adam Benabid, Giulia Nigro, Lucie Peduto

Correspondence

lucie.peduto@pasteur.fr

In brief

After birth, the intestine undergoes villus and vascular remodeling to fulfill nutrient requirement and enhance intestinal barrier function. Peduto and colleagues show that postnatal PDGFRα-dependent intestinal stromal maturation is required to restrain stemness and promote epithelial differentiation and immunoregulation. Failure of stromal maturation leads to decreased postnatal growth and dysregulated intestinal inflammatory and repair responses.

Jacob et al., 2022, Cell Stem Cell *29*, 856–868
May 5, 2022
https://doi.org/10.1016/j.stem.2022.04.005

CellPress

CellPress
OPEN ACCESS

Cell Stem Cell

Article

PDGFRα-induced stromal maturation is required to restrain postnatal intestinal epithelial stemness and promote defense mechanisms

Jean-Marie Jacob,[1] Selene E. Di Carlo,[1,5] Igor Stzepourginski,[1,4,5] Anthony Lepelletier,[1] Papa Diogop Ndiaye,[1] Hugo Varet,[2,3] Rachel Legendre,[2,3] Etienne Kornobis,[2,3] Adam Benabid,[1] Giulia Nigro,[1] and Lucie Peduto[1,6,*]

[1]Stroma, Inflammation & Tissue Repair Unit, Institut Pasteur, Université Paris Cité, INSERM U1224, Paris, France
[2]Transcriptome and Epigenome Platform-Biomics Pole, Institut Pasteur, Université Paris Cité, Paris, France
[3]Bioinformatics and Biostatistics Hub, Institut Pasteur, Université Paris Cité, Paris, France
[4]Present address: Eligo Biosciences, Paris, France
[5]These authors contributed equally
[6]Lead contact
*Correspondence: lucie.peduto@pasteur.fr
https://doi.org/10.1016/j.stem.2022.04.005

SUMMARY

After birth, the intestine undergoes major changes to shift from an immature proliferative state to a functional intestinal barrier. By combining inducible lineage tracing and transcriptomics in mouse models, we identify a prodifferentiation PDGFRα^{High} intestinal stromal lineage originating from postnatal LTβR^{+} perivascular stromal progenitors. The genetic blockage of this lineage increased the intestinal stem cell pool while decreasing epithelial and immune maturation at weaning age, leading to reduced postnatal growth and dysregulated repair responses. Ablating PDGFRα in the LTBR stromal lineage demonstrates that PDGFRα has a major impact on the lineage fate and function, inducing a transcriptomic switch from prostemness genes, such as *Rspo3* and *Grem1*, to prodifferentiation factors, including BMPs, retinoic acid, and laminins, and on spatial organization within the crypt-villus and repair responses. Our results show that the PDGFRα-induced transcriptomic switch in intestinal stromal cells is required in the first weeks after birth to coordinate postnatal intestinal maturation and function.

INTRODUCTION

The intestine constitutes a surface barrier between the host and the external environment. The structural and functional maturation of the intestinal barrier is achieved during the first weeks after birth (Chin et al., 2017). This requires restriction of intestinal stem cells (ISCs) to the crypts and progressive maturation of epithelial and immune intestinal components, overall ensuring digestive and defense functions and a balanced immunity. Notably, crypts containing ISCs are formed around 2 weeks after birth. ISCs continuously generate transit-amplifying (TA) cells that proliferate and differentiate into specialized epithelial lineages including absorptive enterocytes, enteroendocrine cells, antimicrobial secreting Paneth cells, and mucus-producing goblet cells, altogether providing a first line of intestinal defense (van der Flier and Clevers, 2009; Bry et al., 1994). Maintenance of intestinal homeostasis requires localized expression of prostemness and prodifferentiation factors. Stromal cells expressing PDGFRα, which are present in embryonic intestine and essential for intestinal morphogenesis (Karlsson et al., 2000), play an essential role in this process. In the adult lamina propria, PDGFRα^{+} stromal cells, partially coexpressing FoxL1 or Gli1, maintain crypts ISCs by secreting prostemness factors such as Wnt ligands, bone morphogenetic proteins (BMPs) antagonists (Grem1, Grem2), and the ISCs mitogen R-spondins. Ablation of Wnt secretion in PDGFRα^{+}, FoxL1^{+}, or Gli1^{+} stromal cells, as well as genetic depletion of FoxL1^{+} cells, abrogates ISCs proliferation and induces loss of intestinal crypts (Aoki et al., 2016; Degirmenci et al., 2018; Greicius et al., 2018; Shoshkes-Carmel et al., 2018; Batts et al., 2006; Kosinski et al., 2007). BMPs oppose Wnt signaling and promote epithelial differentiation. BMPs are produced by subepithelial PDGFRα^{Hi}Pdpn^{Hi} stromal cells under control of Hedgehog (Hh) ligands, produced by epithelial cells (Stzepourginski et al., 2017; Kosinski et al., 2010; McCarthy et al., 2020). Pdpn^{+} stromal cells play also an essential role in leucocytes migration, positioning, and function (Stzepourginski et al., 2017; Peduto et al., 2009; Perez-Shibayama et al., 2019), suggesting additional immunoregulatory roles.

Postnatal intestinal development requires immune maturation to adapt to microbial density and complexity, food antigens, and potential enteric pathogens. In the small intestine, these changes include homing and expansion of immune populations including myeloid populations such as CD103^{+}CD11b^{+} dendritic cells (DCs) that are essential for neonatal immunity (Lantier et al., 2013). Mostly localized in the intestinal villi, CD103^{+}CD11b^{+} DCs migrate to the mesenteric lymph node (mLN) where they promote differentiation of regulatory T cells (Tregs) in presence

of retinoic acid (RA) and TGF-β. Tregs are key to control the differentiation and activity of effector intestinal T helper subsets (Laffont et al., 2010; Persson et al., 2013; Coombes et al., 2007; Iwata et al., 2004).

One major factor regulating the cross talk between Pdpn$^+$ stromal cells and immune cells is lymphotoxin beta receptor (LTβR). LTβR is required for the development of lymphoid organs and is expressed by different cell types including stromal progenitors with roles in development and inflammation (Lu and Browning, 2014; Bénézech et al., 2010; Fütterer et al., 1998; Bénézech et al., 2012; Krautler et al., 2012). To investigate *in vivo* the role of LTβR$^+$ stromal cells in the intestine, we generated reporter and inducible lineage tracing models for LTβR$^+$ cells. We show that a subset of intestinal PDGFRα$^+$ stromal progenitors expressing LTβR after birth is required for postnatal intestinal epithelial and immune maturation. We demonstrate that development, maturation, and spatial organization of the LTBR stromal lineage requires PDGFRα, and failure for such postnatal stromal maturation leads to reduced postnatal growth, dysregulated intestinal homeostasis, and enhanced susceptibility to inflammation.

RESULTS

Ltbr-expressing cells generate a subepithelial perivascular Pdpn$^+$PDGFRα$^+$ stromal lineage in the first weeks after birth

To investigate LTβR$^+$ stromal progenitors in the intestine, we generated BAC transgenic mice expressing the tetracycline transactivator (tTA) under control of the *Ltbr* promotor (LTBR-tTA mice). By crossing LTBR-tTA mice with tet-regulated Cre (LC1) mice and *Rosa26$^{floxSTOP\text{-}YFP}$* mice (termed LTBR^{YFP} mice, Figure 1A), we performed lineage tracing of LTβR$^+$ cells (in this tet-off system, doxycycline (dox) prevents Cre activation, Figure S1A). In the absence of dox, and consistent with the reported expression of LTβR (Lu and Browning, 2014; Macho-Fernandez et al., 2015), subsets of endothelial, immune, and epithelial cells expressed YFP in the small intestine of adult LTBR^{YFP} mice (Figures S1B and S1C). In addition, we observed around 8% of CD45$^-$CD31$^-$PDGFRα$^+$Pdpn$^+$ stromal cells of the small intestine lamina propria expressing YFP (Figure 1B). YFP was not detected in Pdpn$^-$ stromal cells (Figure S1E). YFP$^+$ stromal cells expressed higher levels of Pdpn and PDGFRα compared with YFP$^-$ stromal cells and were wrapped around subepithelial capillaries with multiple elongated processes, closely adjacent to epithelial cells (Figures 1C, 1D, and S1F). YFP$^+$ stromal cells were mostly enriched in the villi, at the villus bottom and at the junction of villus crypts (Figures 1C and 2A), whereas only rare cells were found around crypts (Figure S1D). Few YFP$^+$ stromal cells were observed in the colon (Figure S1G). The intestine undergoes profound structural and cellular changes in the first weeks after birth (Chin et al., 2017). To investigate when intestinal YFP$^+$ stromal cells develop, we performed FACS analysis of stromal cells in the small intestine of newborn, 2-, 4-, and 8-week-old LTBR^{YFP} mice (Figure 1E). Although Pdpn$^+$ or PDGFRα$^+$ stromal cells are present in the intestine at birth (Stzepourginski et al., 2017), we did not detect YFP$^+$ stromal cells in newborn LTBR^{YFP} mice (Figures 1E and S1H). YFP$^+$ cells strongly expanded between weeks 2 and 4 and then gradually increased until adult age (Figure 1E, green columns). YFP$^+$ stromal population was decreased by the administration of antibiotics, suggesting a role for the microbiota in their development (Figure 1E, blue column). When dox was administrated until week 4, preventing postnatal labeling, only 3% of intestinal stromal cells expressed YFP at 8 weeks (Figure 1E, red column). These results indicate that a major fraction of PDGFRα$^+$ subepithelial stromal cells generated from LTBR$^+$ progenitors develop before weaning age, and low numbers of LTBR$^+$ stromal progenitors are still present in adult intestine. To confirm this hypothesis, we generated a direct LTBR^{GFP} reporter model (Figure 1F). Expression pattern of GFP was consistent with reported LTβR expression (Lu and Browning, 2014; Macho-Fernandez et al., 2015; Figures S1I–S1K). In the intestinal lamina propria, we detected around 1% of PDGFRα$^+$ stromal cells expressing GFP close to the intestinal epithelial layer (Figures 1F and 1G), showing that a small fraction of PDGFRα$^+$LTBR$^+$ stromal progenitors are still present in adult intestine. Analysis of available single-cell datasets of the small intestine confirmed *Ltbr* expression in PDGFRα^{hi} stromal cells (Figure 1H; McCarthy et al., 2020). In addition to subepithelial stromal cells, we observed GFP expression in intestinal endothelial cells (Figure S1K). To investigate lineage relationships, we performed lineage tracing of vascular endothelial (VE)-cadherin$^+$ cells. Consistent with the reported expression of VE-cad by endothelial progenitors and fetal liver hematopoietic progenitors (Kim et al., 2005), a majority of intestinal endothelial cells and a fraction of CD45$^+$ cells were fate mapped in this setting (Figures S1L and S1M). However, no stromal cells were fate mapped, confirming that endothelial and mesenchymal lineages in the intestine have a distinct origin. Altogether, these results show that a subset of PDGFRα$^+$ stromal cells expressing LTβR in the first few weeks after birth generate a subepithelial and perivascular Pdpn$^+$PDGFRα^{High} lineage within the maturing villi, closely adjacent to capillaries, in a process dependent on the microbiota.

The LTβR stromal lineage has a prodifferentiation gene signature at steady state and after injury

To determine whether PDGFRα$^+$YFP$^+$ and PDGFRα$^+$YFP$^-$ stromal cells (Figures 1B and 2A) are transcriptionally different, we performed transcriptome analysis by RNA sequencing (RNA-seq) (Figure 2B). Consistent with their subepithelial localization, YFP$^+$ stromal cells expressed higher levels, compared with YFP$^-$ stromal cells, of genes essential for epithelial cell differentiation, such as *Dll1*, *Bmp4*, *Bmp5*, the Hh receptor *Ptch1*,Hh signaling molecules (*Foxf2*, *Nkx2-3*, and *Gli1*, a transcription factor promoting BMPs expression), and *Frzb* (a Wnt antagonist), and lower levels of genes involved in the maintenance of the epithelial stem cell niche, such as the BMP antagonists *Grem1* and *Grem2*, *Rspo2*, *Rspo3*, *Chrdl1*, *Cd34*, and *Cd81* (Figure 2B; Kosinski et al., 2007, 2010; McCarthy et al., 2020; Stzepourginski et al., 2017). YFP$^+$ stromal cells also overexpressed genes related to RA metabolism (*Rdh10*, *Dhrs4*, *Aldh1a2*, *Aldh1a3*, *Aldha2*, and *Lrat*), which promote intestinal immunity and epithelial differentiation (Oliveira et al., 2018; Lukonin et al., 2020), as well as the chemokines *Ccl11* and *Cxcl14* (Figure 2B). In line with their perivascular subepithelial localization, YFP$^+$ stromal cells expressed higher levels of *Pdgfrb* and *Cspg4*, expressed by pericytes (Di Carlo and Peduto, 2018), as well as components

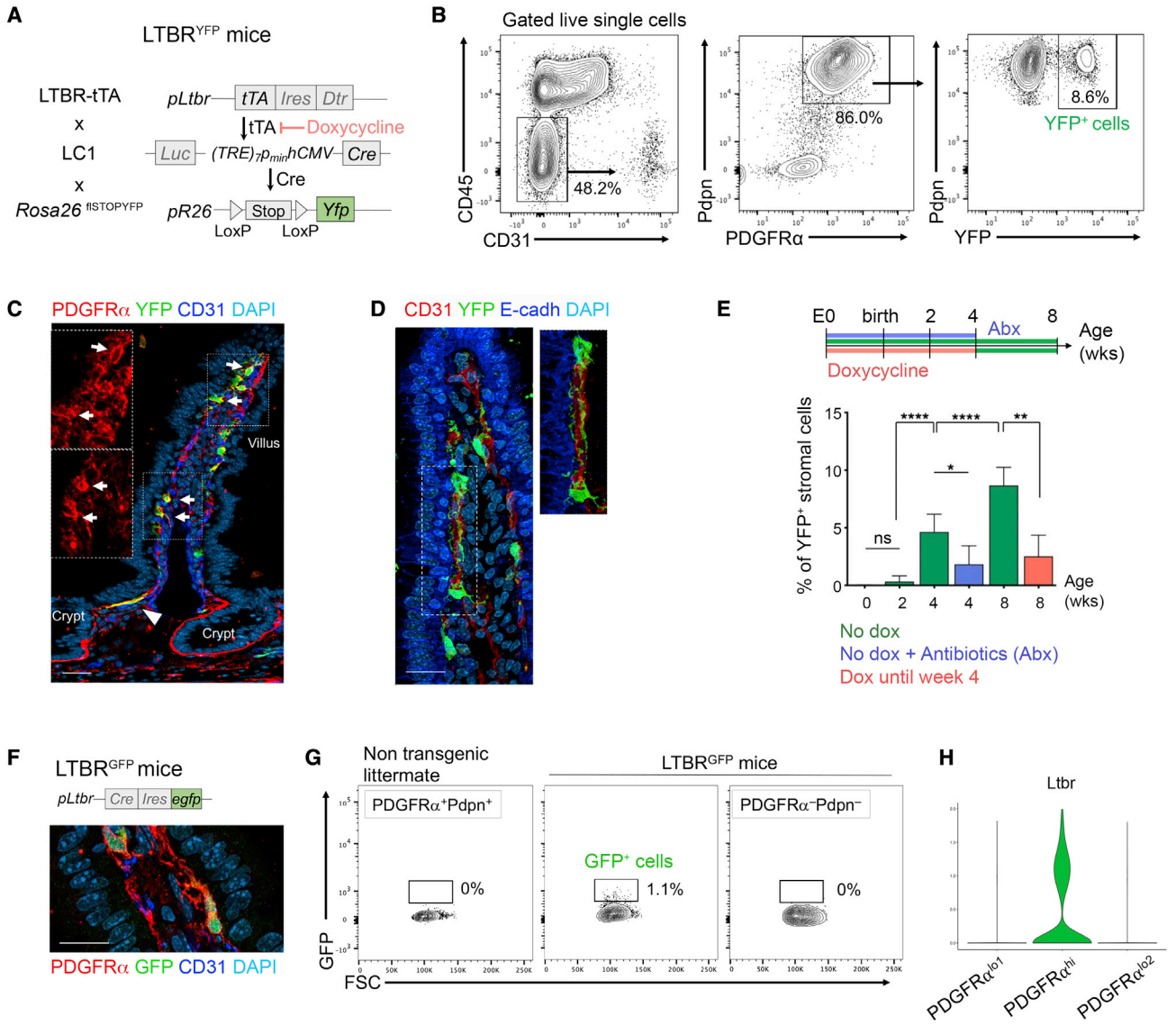

Figure 1. *Ltbr*-expressing cells generate a subepithelial perivascular Pdpn$^+$PDGFRα$^+$ stromal lineage in the first weeks after birth

(A) Strategy for inducible lineage tracing of *Ltbr*-expressing cells.

(B) FACS plots of CD45$^-$CD31$^-$Pdpn$^+$PDGFRα$^+$ stromal cells expressing YFP in the small intestine of LTBR^{YFP} mice. One representative plot of 9 mice from 3 individual experiments is shown.

(C and D) Immunofluorescence analysis of the indicated markers in intestinal sections from LTBR^{YFP} mice. Insets shows high expression of PDGFRα on YFP$^+$ stromal cells (C), wrapped around subepithelial CD31$^+$ capillaries (D).

(E) Experimental setup and frequency of YFP$^+$ cells among intestinal PDGFRα$^+$Pdpn$^+$ stromal cells at the indicated time in LTBR^{YFP} mice. Data are represented as mean ± SD (n = 3–9 from independent experiments).

(F) Immunofluorescence analysis of GFP, CD31, and PDGFRα in intestinal sections from LTBR^{GFP} mice.

(G) FACS plot of CD45$^-$CD31$^-$ stromal cells expressing GFP in the small intestine of LTBR^{GFP} mice or nontransgenic littermate. One representative plot of 3 individual experiments is shown. (H) Expression of *Ltbr* in intestinal PDGFRα$^+$ stromal cells, analyzed from single-cell dataset (GSE130681) (McCarthy et al., 2020).

In (C), (D), and (F), representative images of 3 independent experiments are shown. *p < 0.05, **p < 0.01, ****p < 0.0001, as determined by unpaired Student's t test. ns (not significant). Scale bars, 20 μm. Dapi stains nuclei.

See also Figure S1.

of the basement membrane including *Col4a1*, *Col4a2*, *lama1*, *lamb1*, *lamc1*, and genes coding for collagen VI (*Col6a1*, *a2*, *a4*, and *a5*), which anchors structures to the surrounding ECM (Groulx et al., 2011; Kuo et al., 1997). Immunofluorescence analysis confirmed localization of YFP$^+$ cells within the ColIV$^+$ basement membrane (Figure S2A). In contrast, YFP$^-$ stromal cells expressed higher level of proinflammatory cytokines and chemokines *Il6*, *Ccl2*, *Cxcl1*, *Cxcl2*, and *Cxcl10*, as well as

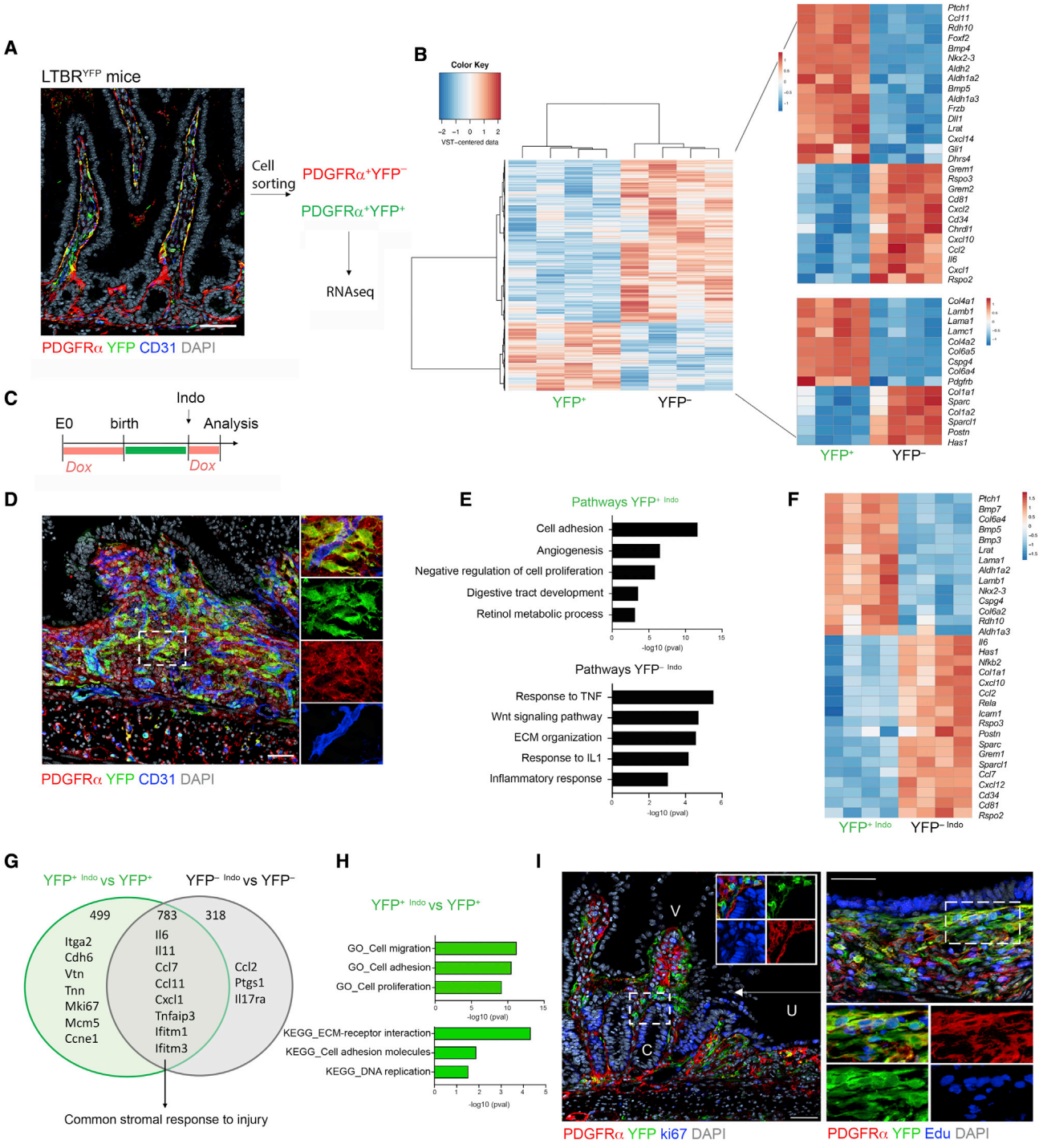

Figure 2. The LTBR stromal lineage has a prodifferentiation gene signature at steady state and after injury

(A) Immunofluorescence analysis of the indicated markers in intestinal sections from LTBR^{YFP} mice.

(B) Differential gene expression analysis by RNA-seq, and heatmap of selected genes in PDGFRα^{+}YFP^{+} and PDGFRα^{+}YFP^{-} stromal cells isolated from LTBR^{YFP} mice (n = 4).

(C) Experimental strategy for indomethacin treatment.

(D) Immunofluorescence analysis of the indicated markers in intestinal sections of LTBR^{YFP} mice treated with indomethacin as indicated in (C).

(E and F) Enriched pathways (gene ontology) (E) and heatmap of selected genes (F) in PDGFRα^{+}YFP^{+} (YFP^{+Indo}) and PDGFRα^{+}YFP^{-} (YFP^{-Indo}) stromal cells isolated from the ulcers of indomethacin-treated LTBR^{YFP} mice (n = 4).

(G) Overlap of upregulated genes (FC > 2) in inflamed YFP^{+} ^{Indo} and YFP^{-} ^{Indo} stromal cells, versus their respective population at steady state. Representative genes are shown.

(legend continued on next page)

structural and matricellular proteins involved in tissue remodeling and inflammation such as *Col1a1*, *Col1a2*, *Sparc*, *Postn*, and *Has1* (Figure 2B). To investigate the fate of the postnatal LTBR^{+} stromal lineage during injury, we injected indomethacin, which induces intestinal ulcers (Sigthorsson et al., 2002), in LTBR^{YFP} mice (Figure 2C). Of note, we added dox from the time of injury to prevent labeling of cells that might upregulate LTBR after injury. We observed that YFP^{+} cells massively expanded in the ulcer's, mostly in the upper part of the lamina propria, and were still loosely connected to blood vessels, surrounded by PDGFRα^{+} stromal cells not derived from LTBR lineage (YFP^{-}) (Figure 2D). Expansion of YFP^{+} cells was specific to injured regions and was not observed in noninjured zones of indomethacin-treated mice (Figure S2B). Differential expression analysis of PDGFRα^{+}YFP^{+} and PDGFRα^{+}YFP^{-} stromal cells isolated from ulcers indicated that YFP^{+} and YFP^{-} populations maintain a distinct gene signature after injury. Accordingly, injury-induced YFP^{+} cells (YFP$^{+\ Indo}$) were enriched in GO terms related to cell adhesion, angiogenesis, basement membrane matrix proteins, prodifferentiation factors, and genes related to RA synthesis (Figures 2E and 2F). In contrast, YFP^{-} cells (YFP$^{-\ Indo}$) were enriched in genes promoting Wnt signaling, proinflammatory cytokines, responses to TNF-α and IL1, leukocyte chemoattractants such as *Ccl2* and *Ccl7*, and matrix proteins with roles in fibrosis and inflammation such as *Col1a1*, *Postn*, *Sparc*, and *Has1* (Jiang et al., 2007; Ng et al., 2013; Koh et al., 2016; Figures 2E and 2F). Although not unique to a stromal subset, YFP^{-} expressed *Il1r1* (Figure S2C), involved in Rspo3 mediated stromal coordination of intestinal repair after dextran sodium sulfate (DSS) (Cox et al., 2021). We further investigated how gene expression change in each lineage in response to injury. We observed that although YFP^{-} cells overall express higher levels of proinflammatory molecules compared with YFP^{+} cells, both injury-activated YFP^{+} PDGFRα^{+} and YFP^{-} PDGFRα^{+} stromal lineages upregulated cytokines, chemokines, and IFN-induced genes including *Il6*, *Il11*, *Cxcl1*, *Ccl7*, and *Ifitm3* compared with homeostasis, suggesting a common stromal response related to innate immunity (Figure 2G). In addition, injury-activated YFP^{+} cells specifically upregulated genes regulating cell matrix adhesion, cell migration, and proliferation (Figures 2G and 2H) while downregulating genes involved in Hh signaling such as *Gli1*, compared with YFP^{+} cells at steady state (Figure S2D). In line with this observation, injury-activated YFP^{+} cells rapidly detached from the damaged villus epithelium, the major producer of Hh ligands, accumulated at the bottom of the villus and massively proliferated and migrated within the wound in the first few days after injury (Figure 2I). Altogether, these results show that the postnatal YFP^{+}PDGFRα^{+} stromal lineage is enriched in factors essential for epithelial differentiation/ integrity and immunoregulation, whereas YFP^{-}PDGFRα^{+} stromal cells express genes involved in the maintenance of the ISCs niche, matrix remodeling, and inflammation. After injury, YFP^{+}PDGFRα^{+} cells, which are strategically localized in the villi to sense damage, rapidly proliferate and migrate within the wound.

Conditional ablation of PDGFRα in the LTBR lineage restrains postnatal intestinal maturation

Our results indicate that the LTBR lineage develops in the first few weeks after birth, a key period for intestinal maturation (Noah et al., 2011) and expresses high levels of PDGFRα (Figures 1C and 1H), which plays fundamental roles in cell growth and differentiation (Hoch and Soriano, 2003; Olson and Soriano, 2009). To investigate the role of PDGFRα in the LTBR lineage, we crossed LTBR-tTA mice to tet-regulated Cre (LC1) mice and PDGFR$\alpha^{fl/fl}$ mice (LTBR$^{\triangle PDGFRa}$ mice; Figure 3A), and removed dox at birth to ablate postnatal PDGFRα in YFP^{+} cells (Figure 3B). We observed that LTBR$^{\triangle PDGFRa}$ pups gained significantly less weight starting from week 2 compared with their WT littermates (Figure 3C), which is when intestinal YFP^{+} stromal cells develop (Figure 1E). In the intestine of LTBR$^{\triangle PDGFRa}$ mice, we did not observe major differences in the intestinal length, overall structure, and gut-associated lymphoid tissues compared with 4-week-old littermates (Figures 3D, S3A, and S3B). In contrast, we observed a significant increase in Olfm4^{+} cells, a marker for ISCs (Schuijers et al., 2014; Figure S3C), as well as in Lgr5^{+} ISCs (Figure S3D), and EdU^{+} proliferating epithelial cells in LTBR$^{\triangle PDGFRa}$ mice compared with WT littermates, although goblet cells were decreased (Figure 3D). No differences were detected in Paneth cells and Tuft cells (Figures 3D and S3E). Consistent with an increase in the stem cells pool, epithelial cells isolated from LTBR$^{\triangle PDGFRa}$ mice had increased expression of transcripts coding for the ISCs markers *Olfm4*, *Lgr5* (Hadis et al., 2011; van der Flier et al., 2009; Barker et al., 2007), and *EphB3*, a target of Wnt signaling (Figure 3E; Qi et al., 2017), compared with epithelial cells isolated from the intestine of WT littermate mice. In addition, epithelial cells isolated from LTBR$^{\triangle PDGFRa}$ mice showed decreased expressions of *Klf4* and *Muc2*, expressed by goblet cells, of *Sucrase isomaltase* (*Sis*), expressed in mature enterocytes, as well as *Tff3* (mainly produced by goblet cells) and *Tjp2* (ZO-2) that have essential roles in maintenance of epithelial tight junctions (Figure 3E). Of note, Sis is essential for digestion of dietary carbohydrates (Muncan et al., 2011), suggesting that a defect in enterocyte maturation might be involved in the lower weight of LTBR$^{\triangle PDGFRa}$ mice. In line with the proliferative phenotype, we observed that stromal cells isolated from LTBR$^{\triangle PDGFRa}$ mice expressed lower levels of BMPs and Wnt antagonists and higher levels of prostemness signals such as *Grem2* and *Chrdl1* (Figure S3F). As postnatal intestinal maturation is concomitant to immune recruitment, we analyzed the frequency of lamina propria immune cells in LTBR$^{\triangle PDGFRa}$ mice. We did not observe significant differences in B cells, T helper subsets, CD8^{+} T cells, ILCs, or major populations of myeloid cells in LTBR$^{\triangle PDGFRa}$ mice (Figure S3G). In contrast, we observed a significant decrease in intestinal CD103^{+}CD11b^{+} DCs (Figure 3F), which expressed RA, a major factor regulating intestinal Tregs homeostasis (Tanoue et al., 2016; Figure S4A). Intestinal CD103^{+}CD11b^{+} DCs migrate to the mLN and induce differentiation of Tregs (Coombes et al., 2007; Ruane and Lavelle, 2011; Schulz et al., 2009). Consistent

(H) Enriched pathways in YFP^{+Indo} versus YFP^{+} stromal cells excluding overlap genes.
(I) Immunofluorescence analysis of the indicated markers in intestinal sections of LTBR^{YFP} mice treated with indomethacin for 1 day (left) or 4 days (right).
In (A), (D), and (I), one representative image from 3 individual experiments is shown. U, Ulcer; C, Crypt; V, Villus. Scale bars, 50 μm.
See also Figure S2.

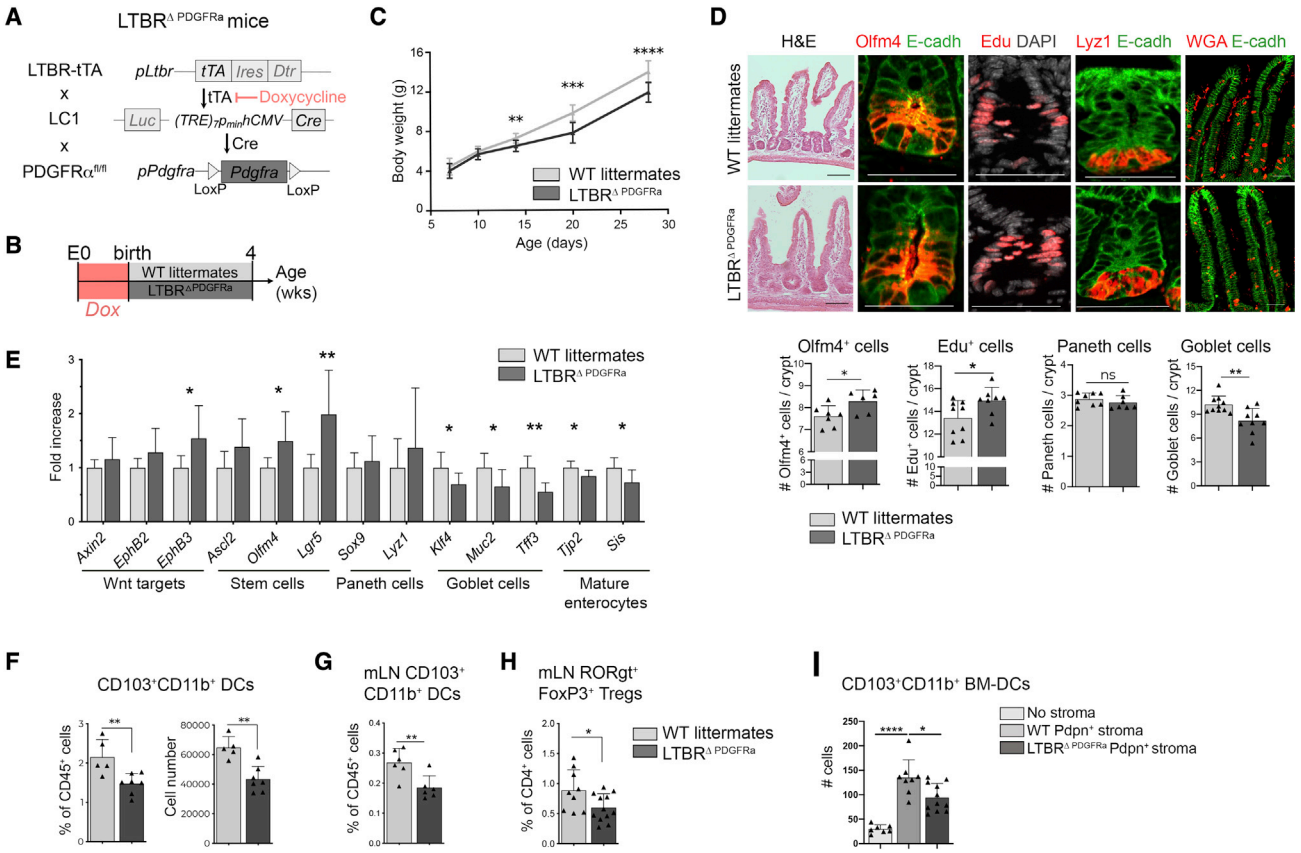

Figure 3. Conditional ablation of PDGFRα in the LTBR lineage restrains postnatal intestinal maturation

(A) Strategy for conditional ablation of PDGFRα in the LTBR lineage.

(B) Experimental setup in (C)–(H).

(C) Body weight of LTBR$^{\Delta PDGFRa}$ mice and WT littermates at the indicated age after birth. n = 7–10 from at least 3 independent experiments. The line connects the mean ± SD of each time point.

(D) H&E staining and immunofluorescence analysis of the indicated markers on intestinal sections. N = 6–9 mice from 2 to 5 independent experiments.

(E) Expression of the indicated genes, measured by qRT-PCR, on the epithelial fraction. n = 8–10 from 3 independent experiments.

(F) Frequency (left) and cell number (right) of intestinal CD103$^+$CD11b$^+$ DCs, measured by FACS. n = 5–7 mice from 2 independent experiments, representative of 3.

(G and H) Frequency of CD103$^+$CD11b$^+$ DCs (G) and RORgt$^+$Foxp3$^+$ T cells (H) in the mesenteric lymph node (mLN). n = 4–5 mice from 2 independent experiments (G) and n = 10–13 from 4 independent experiments (H).

(I) CD103$^+$CD11b$^+$ BM derived DCs, measured by FACS, cultivated with Pdpn$^+$ stromal cells isolated by FACS from the small intestine of 4-week-old LTBR$^{\Delta PDGFRa}$ mice or WT littermates. n = 8–11 from 4 independent experiments.

In (D)–(I), data are represented as mean ± SD. ns (not significant). *p < 0.05, **p < 0.01,*** < 0.001, ****p < 0.0001 as determined by unpaired Student's t test. Scale bars, 50 μm.

See also Figures S3 and S4.

with a decrease of intestinal CD103$^+$CD11b$^+$ DCs, we observed a decrease of CD103$^+$CD11b$^+$ DCs in the mLN of LTBR$^{\Delta PDGFRa}$ mice (Figure 3G), as well as of RORgt$^+$FoxP3$^+$ Tregs induced in the mLN (Figure 3H) and a trend of decrease of intestinal RORgt$^+$FoxP3$^+$ Tregs (data not shown). We observed that a majority of intestinal CD11c$^+$CD103$^+$ DCs were closely adjacent to YFP$^+$ cells (Figures S4B and S4C), suggesting a cross talk stroma-DCs. Consistent with this hypothesis, Pdpn$^+$ stromal cells isolated from LTBR$^{\Delta PDGFRa}$ mice were less efficient than WT Pdpn$^+$ stroma to maintain CD103$^+$CD11b$^+$ BM-DCs *in vitro* (Figure 3I). Altogether, these data show that PDGFRα expression in the LTBR stromal lineage is required for postnatal mice growth and intestinal epithelial and immune maturation.

LTBR$^{\Delta PDGFRa}$ mice display dysregulated responses to intestinal injury

Our results show that LTBR$^{\Delta PDGFRa}$ mice have dysregulated intestinal epithelial and immune postnatal maturation. To determine whether such dysregulation has an impact on inflammation, we treated 4-week-old LTBR$^{\Delta PDGFRa}$ mice and littermate WT mice with DSS (Figure 4A). We did not observe major structural changes in the small intestine of DSS-treated LTBR$^{\Delta PDGFRa}$ mice and littermate mice, consistent with previous reports showing that DSS-induced ileal inflammation has minor epithelial damage (Sartor, 1997). Nevertheless, we detected higher expression of *Pdgfa* in the small intestine of DSS-treated LTBR$^{\Delta PDGFRa}$ mice and littermates compared with nontreated

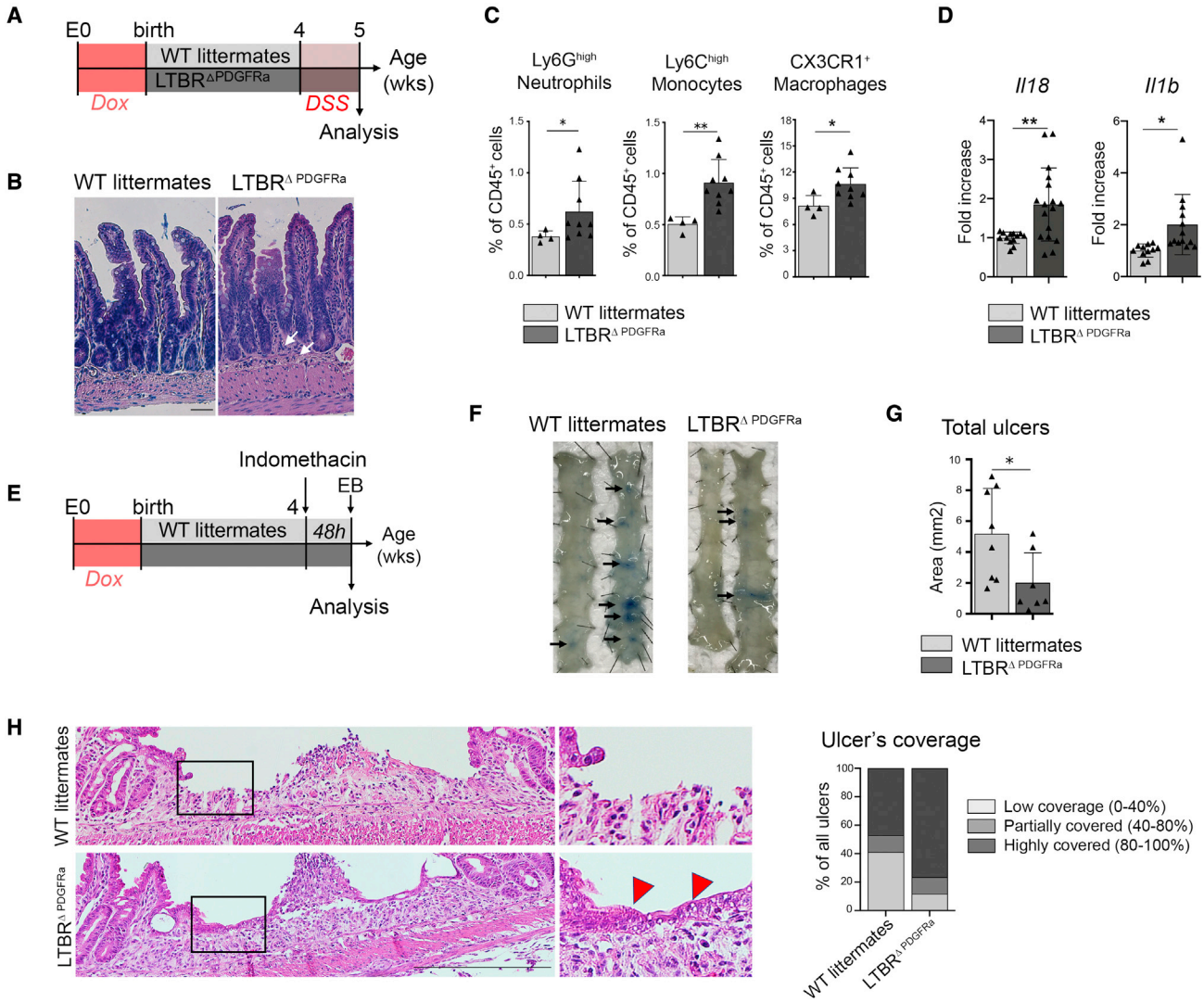

Figure 4. LTBR$^{\Delta PDGFRa}$ mice display dysregulated response to intestinal injury

(A) Experimental strategy for DSS treatment in (B)–(D).

(B) H&E coloration of intestinal sections of DSS-treated LTBR$^{\Delta PDGFRa}$ mice and WT littermates. Arrows indicates highly infiltrated zones. Scale bars, 50 μm.

(C) Frequency of the indicated immune populations in the small intestine of DSS-treated LTBR$^{\Delta PDGFRa}$ mice and WT littermates. n = 4–9 from 2 independent experiments.

(D) Expression of the indicated transcripts, as measured by qRT-PCR, in the small intestine of DSS-treated LTBR$^{\Delta PDGFRa}$ mice and WT littermates. n = 13–17 from 3 independent experiments.

(E) Experimental strategy for indomethacin treatment in (F)–(H).

(F and G) Images of indomethacin induced intestinal ulcers (stained with Evan's Blue, black arrows in F), and measure of ulcers area (G) in LTBR$^{\Delta PDGFRa}$ mice and WT littermates. Representative images from 3 independent experiments are shown (n = 7–8).

(H) H&E coloration (left, arrowheads indicate epithelial coverage) and quantification of ulcer's coverage by epithelial cells (right). A minimum of 20 ulcers were analyzed from 14 mice from 2 independent experiments, and one representative image is shown. Scale bars, 100 μm.

In (C), (D), and (G), data are represented as mean ± SD. *$p < 0.05$, **$p < 0.01$ as determined by unpaired Student's t test. EB: Evan's Blue.

See also Figure S4.

mice, suggesting a role for PDGF in inflammation (Figure S4D). We further observed intestinal length shortening (Figure S4E) and increased leucocyte infiltration and thickness of the smooth muscle layer in the small intestine of DSS-treated LTBR$^{\Delta PDGFRa}$ mice (Figure 4B), consistent with increased inflammation. Accordingly, the frequency of neutrophils, Ly6C^{High} monocytes, and inflammatory macrophages in the small intestine of LTBR$^{\Delta PDGFRa}$ mice was increased following DSS (Figure 4C), as well as expression of the proinflammatory cytokines *Il1b* and *Il18* (Figure 4D), but not at steady state (Figure S4F). Tregs were not significantly impacted (Figure S4G). As we did not observe damage to the epithelium in DSS-induced ileitis, we injected indomethacin in 4-week-old LTBR$^{\Delta PDGFRa}$ mice and WT littermates (Figure 4E) to further investigate epithelial repair.

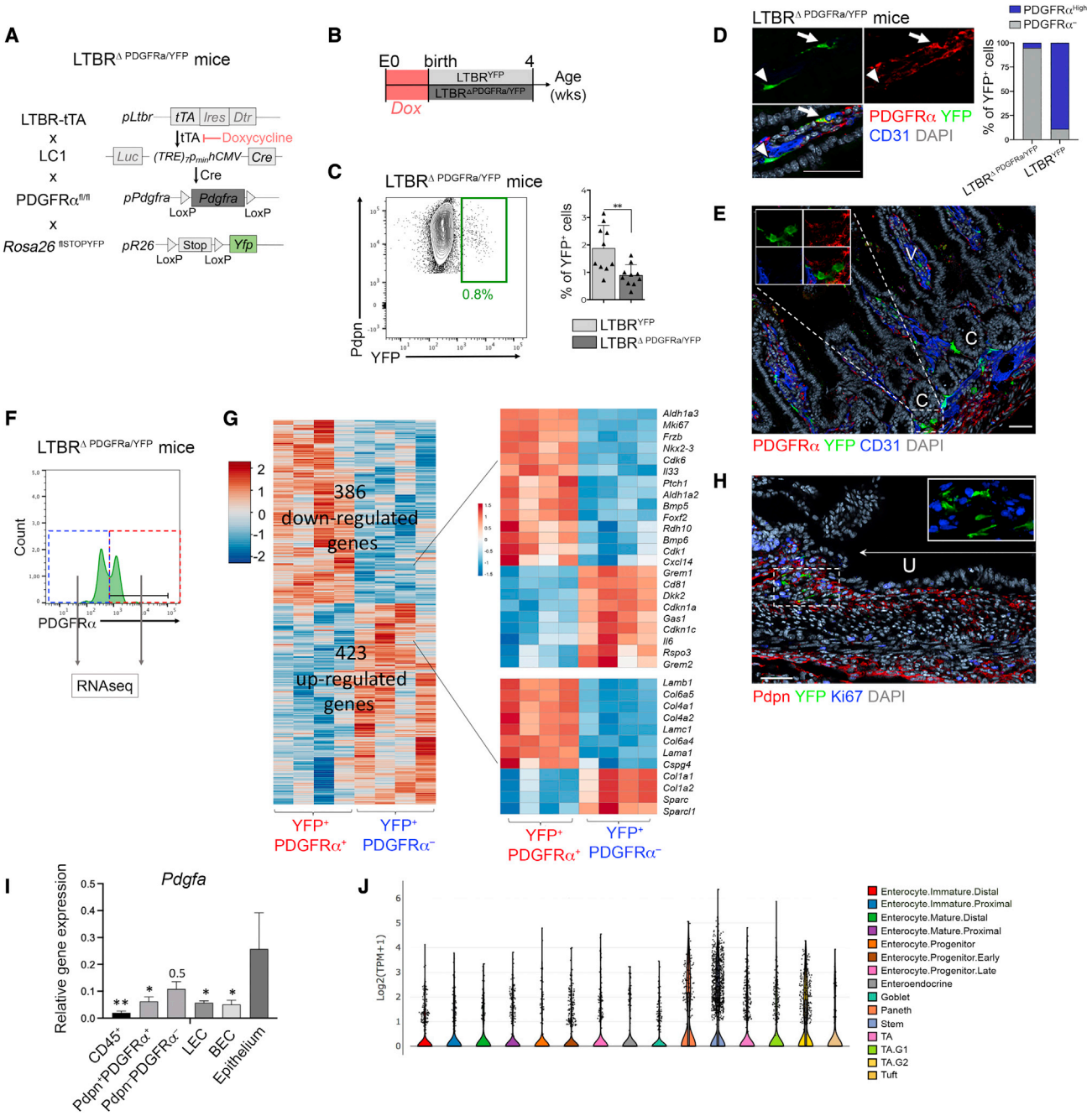

Figure 5. PDGFRα induces a major transcriptomic switch in the LTBR stromal lineage

(A) Strategy for the generation of LTBR$^{\Delta PDGFRa/YFP}$ mice.

(B) Experimental setup in (C) and (D).

(C) FACS plot and percentage of CD45$^-$CD31$^-$ stromal cells expressing YFP in the small intestine of the indicated mice treated as in (B); n = 10 from 4 independent experiments.

(D) Immunofluorescence analysis of the indicated markers in intestinal sections from LTBR$^{\Delta PDGFRa/YFP}$ mice (left) and percentage of YFP$^+$PDGFRα^{High} stromal cells (arrow) and YFP$^+$PDGFRα$^-$ (arrowhead) in the indicated mice (right). Quantification was done on 30 images from 4 independent experiments.

(E) Immunofluorescence analysis of the indicated markers in intestinal sections from 4-week-old LTBR$^{\Delta PDGFRa/YFP}$ mice.

(F) Mean fluorescence intensity (MFI) of PDGFRα expression in YFP$^+$ stromal cells from LTBR$^{\Delta PDGFRa/YFP}$ mice. One representative plot is shown (n = 6–12).

(G) RNA-seq analysis and heatmap of selected genes differentially expressed in YFP$^+$PDGFRα$^+$ stromal cells versus YFP$^+$PDGFRα$^-$ stromal cells isolated from LTBR$^{\Delta PDGFRa/YFP}$ mice, n = 4 mice.

(H) Immunofluorescence analysis of the indicated markers in intestinal sections of 4-week-old LTBR$^{\Delta PDGFRa/YFP}$ mice treated with indomethacin for 4 days.

(I) Expression of *Pdgfa* measured by qRT-PCR in the indicated populations isolated by FACS from the small intestine of WT mice. n = 4–6 from 2 independent experiments.

(legend continued on next page)

We observed decreased ulceration surface in the small intestine of LTBR$^{\triangle PDGFRa}$ mice compared with WT littermate mice (Figures 4F and 4G). Histological analysis indicated that the majority of ulcers lacked epithelial coverage in WT littermate mice, although similar size ulcers in LTBR$^{\triangle PDGFRa}$ mice were mostly covered by epithelial cells (Figure 4H, red arrowheads), suggesting improved regeneration. Overall, these results show that expression of PDGFRα in the LTBR stromal lineage is required to regulate postnatal repair and inflammatory intestinal responses.

PDGFRα induces a major transcriptomic switch in the LTBR stromal lineage

To investigate the underlying mechanism, we engineered a genetic model to trace YFP$^+$ cells in postnatal LTBR$^{\triangle PDGFRa}$ mice. To that aim, we crossed LTBR$^{\triangle PDGFRa}$ mice to *Rosa26*$^{floxSTOP-YFP}$ reporter mice (LTBR$^{\triangle PDGFRa/YFP}$ mice; Figure 5A), removed dox at birth, and analyzed the small intestine of 4-week-old LTBR$^{\triangle PDGFRa/YFP}$ mice (Figure 5B). Compared with LTBR^{YFP} mice, which have WT expression of PDGFRα, YFP$^+$ stromal population in LTBR$^{\triangle PDGFRa/YFP}$ mice was decreased by 50% (Figure 5C), showing that the deletion of PDGFRα from YFP$^+$ stromal cells regulate their development or survival. Consistent with specific expression of PDGFRα in stromal cells (Figure S5A), YFP$^+$ endothelial and YFP$^+$ immune cells were not affected (Figure S5B). Less than 5% of YFP$^+$ cells still present in the small intestine of LTBR$^{\triangle PDGFRa/YFP}$ mice expressed high levels of PDGFRα (Figure 1C), confirming efficient deletion of PDGFRα (Figure 5D, arrows indicate YFP$^+$PDGFRα^{High} stromal cells, and arrowheads indicates YFP$^+$PDGFRα$^-$ stromal cells). Most YFP$^+$ cells in the small intestine of LTBR$^{\triangle PDGFRa/YFP}$ mice were PDGFRα$^-$ Pdpn^{low}, had lost their subepithelial position, and accumulated in the lower part of the lamina propria (Figures 5E and S5C). As a fraction of YFP$^+$ cells still expressed low but detectable levels of PDGFRα, consistent with gradual excision (Figures 5F and S5D), we performed RNA-seq to investigate molecular changes occurring in a single stromal lineage, *in vivo*, following deletion of PDGFRα. We identified a total of 809 differentially regulated genes between YFP$^+$PDGFRα$^+$ and YFP$^+$PDGFRα$^-$ stromal cells isolated from the small intestine of LTBR$^{\triangle PDGFRa/YFP}$ mice, indicating that the removal of PDGFRα has a major impact on the transcriptome of the LTBR stromal lineage. Consistent with a role in cell proliferation, YFP$^+$ cells lacking PDGFRα downregulated genes involved in cell proliferation (*Mki67*, *Cdk1*, and *Cdk6*) and upregulated genes involved in cell cycle arrest (*Gas1*, *Cdkn1a*, and *Cdkn1c*). Accordingly, PDGF-AA increased expression of proliferation and prosurvival markers such as *Mki67*, *Cdk1*, and *Bcl2* in PDGFRα$^+$ stromal cells *in vitro* (Figure S5E). In addition, major genes essential for epithelial differentiation such as *Bmp5*, *Bmp6*, *Ptch1*, and *Frzb* and enzymes involved in RA synthesis such as *Aldh1a2*, *Aldh1a3*, and *Rdh10* were downregulated in YFP$^+$PDGFRα$^-$ stromal cells, compared with YFP$^+$PDGFRα$^+$ stromal cells, whereas BMP inhibitors *Grem1* and *Grem2* and Wnt regulators *Dkk2*, *Rspo3*, and *Cd81* were upregulated (Figure 5G). Other downregulated genes included *Il33*, which promotes epithelial differentiation and type 2 Immunity (Allen and Sutherland, 2014; Mahapatro et al., 2016), as well as components of the basement membrane and ECM anchoring proteins such as laminins, collagen IV, and collagen VI, respectively. In contrast, ECM fibrillar collagens such as *Col1a* and matricellular proteins *Sparc* and *Sparcl1* were upregulated. These data demonstrate that PDGFRα has a predominant role in the survival, localization, and proper maturation of the LTBR stromal lineage and overall shaping of the subepithelial niche. To further determine whether PDGFRα is required for the expansion of the YFP lineage during injury (Figure 2D), we injected indomethacin in LTBR$^{\triangle PDGFRa/YFP}$ mice. We observed rare YFP$^+$ki67$^-$ cells that remained within the ulcer's borders and did not migrate and expand within the injured zone (Figure 5H), as in LTBR^{YFP} mice (Figure 2D), demonstrating that PDGFRα is required for the function of the LTBR stromal lineage after injury. Finally, as PDGF-AA is one of the main ligands of PDGFRα, we investigated *Pdgfa* expression in intestinal populations. We observed that *Pdgfa* is expressed at higher levels in intestinal epithelial cells compared with other cells of the lamina propria, although perivascular cells such as pericytes and vascular smooth muscle cells also express detectable levels (Figures 5I and S5F). Single-cell analysis of the small intestinal epithelium (Haber et al., 2017) further indicated that most intestinal epithelial subsets express *Pdgfa*, suggesting a major role for epithelial cells in shaping their own subepithelial niche (Figure 5J). As ISCs and TA cells are major expressers of *Pdgfa*, it suggests a feedback control mechanism to control stem cell proliferation. Of note, additional ligands of PDGFRα, such as *Pdgfc*, are expressed by intestinal smooth muscle cells (Figure S5F). As *Pdgfb* is expressed by blood endothelial cells (Figure S5G), this further suggests tight control of YFP$^+$ cells, which also express *Pdgfrb* (Figure 2B), by PDGFR ligands availability and proximity within the intestine. In line with their postnatal development, we detected a peak of expression of *Pdgfa* and *Pdgfb* in the small intestine the first week after birth, whereas *Pdgfc* increased between weeks 1 and 3 (Figure S5H). Overall, these data show that PDGFRα is required for maturation, localization, and function of the postnatal LTBR lineage in the small intestine at steady state and after tissue damage.

DISCUSSION

Postnatal development of the intestinal barrier requires coordinated epithelial and immune maturation. Here, we show that a subset of intestinal PDGFRα$^+$ stromal progenitors expressing LTβR after birth play an essential role in this process by generating a prodifferentiation and immunoregulatory stromal niche within the growing villus. We demonstrate that development, maturation, and spatial organization of the LTBR lineage requires

(J) Expression of *Pdgfa* in single cells of the small intestinal epithelium (https://singlecell.broadinstitute.org/single_cell/study/SCP44/small-intestinal-epithelium) (Haber et al., 2017).

In (C) and (I), data are represented as mean ± SD. In (E) and (H), a representative image from 3 to 4 independent experiments is shown. *$p < 0.05$, **$p < 0.01$, as determined by unpaired Student's t test. U, Ulcer; C, Crypt; V, Villus; LECs, lymphatic endothelial cells; BECs, blood endothelial cells. Scale bars, 50 μm.
See also Figure S5.

PDGFRα, and failure for such postnatal stromal maturation leads to reduced postnatal growth, dysregulated intestinal homeostasis, and response to injury.

In contrast to PDGFRα$^+$ stromal cells that are already present in fetal intestine, the LTBR lineage develops and expands in the first few weeks after birth in the small intestine. The postnatal period coincides with major structural and functional intestinal changes, including restriction of proliferative epithelial cells within the crypts, promotion of epithelial differentiation along the villi, as well as homing and differentiation of immune populations essential for intestinal immunity (Bry et al., 1994; Chin et al., 2017). Transcriptomic profiling indicated that the LTBR lineage overexpresses several soluble and structural factors essential for this process. In agreement with previous reports (McCarthy et al., 2020), the LTBR lineage expresses high levels of PDGFRα, Pdpn, and BMPs. In addition, the LTBR stromal lineage is enriched in transcripts coding for key factors in cell differentiation, such as RA, components of the basement membrane and ECM anchoring meshwork, as well as pericyte markers, consistent with their perivascular localization (Powell et al., 2011). As the LTBR lineage is wrapped around subepithelial capillaries, it is localized in a strategic position to sense and respond to both epithelial cells and circulating factors. In contrast, PDGFRα$^+$ stromal cells not derived from LTβR$^+$ progenitors overexpressed factors promoting stem cells maintenance, including BMP inhibitors, the Wnt signaling coactivators *Rspo2*/*Rspo3*, the pericryptal stromal markers *Cd81* and *Cd34*, as well as chemokines, cytokines, and ECM proteins with essential roles in matrix remodeling and inflammation (Stzepourginski et al., 2017; McCarthy et al., 2020; Hageman et al., 2020). Consistent with the massive colonization of the intestine by the microbiota at birth, we show that the microbiota promotes development of the LTBR lineage. It remains to be assessed whether this effect is direct or indirect, as the microbiota regulates several intestinal components including immune cells, epithelial cells, and the vasculature (Al Nabhani and Eberl, 2020; Reinhardt et al., 2012; Schirbel et al., 2013; Stappenbeck et al., 2002), which might impact on stromal cells.

Our data are in agreement with previous reports showing that PDGFRα and PDGF-AA have an essential role in intestinal morphogenesis (Karlsson et al., 2000) and further show that postnatal intestinal maturation requires differentiation of a subset of PDGFRα$^+$ stromal cells to restrict ISC proliferation and promote adult intestinal barrier function. This requires soluble factors that antagonize Wnts as well as other local and structural factors such as matrix proteins constituting the basement membrane, which is required for proper epithelial differentiation and integrity (Gjorevski et al., 2016; Groulx et al., 2011; Simon-Assmann et al., 1998), and RA, which has key roles in epithelial differentiation and intestinal immunity (Oliveira et al., 2018; Lukonin et al., 2020). Accordingly, RA signaling plays an essential role in epithelial homeostasis by regulating exit from epithelial regenerative state and driving enterocyte differentiation (Lukonin et al., 2020) and is a determinant factor inducing anti-inflammatory CD103$^+$CD11b$^+$ RA-producing DCs in the small intestine (Bakdash et al., 2015; Agace and Persson, 2012). Although RA is also produced by epithelial cells, our observations that a majority of CD103$^+$CD11b$^+$ DCs are localized in close proximity to YFP$^+$ cells and that stromal cells isolated from LTBR$^{\Delta PDGFRa}$ mice have a decreased capacity to maintain CD103$^+$CD11b$^+$ DCs suggests that the subepithelial stromal niche plays a role in this process. In line with our results, intestinal Pdpn$^+$ stromal cells produce RA and induce RA synthesis in DCs *in vitro* (Vicente-Suarez et al., 2015).

We further demonstrate that PDGFRα is required for the fate and function of the LTBR lineage at steady state and after injury. Conditional knockout of PDGFRα in the postnatal LTBR lineage results in a 50% decrease in the cell population, consistent with previous reports showing a role for PDGFRα in mesenchymal cell survival and proliferation (Karlsson et al., 2000; Li and Hoyle, 2001; Zhuo et al., 2006). In addition, the LTBR stromal lineage lacking PDGFRα had lost its subepithelial localization within the villi, in line with major transcriptomic changes showing downregulation of BMPs, Hh signaling, collagen IV, and laminins, although overexpressing prostemness genes such as BMP antagonists, as well as proinflammatory and profibrotic genes such as *Il6*, *Sparc*, and *Col1a*. In agreement with these findings, BMP4 and BMP5 expression is decreased in the lamina propria of newborn PDGFRα KO mice (Karlsson et al., 2000), and constitutive activation of PDGFRα signaling induces fibrosis (Olson and Soriano, 2009). PDGFRα also promoted expression of genes with immunomodulatory roles, such as RA enzyme synthesis and IL-33, a cytokine inducing type 2 immunity and involved in differentiation of goblet cells (Oliveira et al., 2018; Mahapatro et al., 2016), indicating that PDGFRα stromal expression has a major impact on tissue function. Our *in vivo* data showing increased epithelial proliferation, decreased generation of goblet cells, and dysregulation of DCs are consistent with these transcriptomic changes. Overall, these data show that PDGFRα is, directly or indirectly, required for development, maturation, and spatial organization of the postnatal LTBR stromal lineage. As the LTBR lineage revert to an immature prostemness phenotype in the absence of PDGFRα, both at the transcriptomic level and localization, our data support the hypothesis that a subset of postnatal PDGFRα$^+$ stromal cells expressing LTβR acquire prodifferentiation and immunoregulatory functions to ensure postnatal intestinal maturation. These data also show that stromal cells function is impacted by cross talk with their microenvironment through PDGFRα.

We further show that LTBR$^{\Delta PDGFRa}$ mice have dysregulated repair responses. These data are consistent with dysregulation of the stromal niche, as the LTBR lineage did not develop properly in absence of PDGFRα, and the remaining PDGFRα$^-$ LTBR lineage reverted to an immature phenotype (Figure 5). We hypothesized that the defect of maturation of the LTBR lineage does not counterbalance the inflammatory/regenerative signals produced by PDGFRα$^+$YFP$^-$ stromal cells, resulting in dysregulated regenerative and inflammatory responses. These data are in line with increasing evidence that similar pathways are engaged in inflammation and regeneration (Hageman et al., 2020) and show that PDGFRα$^+$ intestinal stromal cells play an essential role in this cross talk. In agreement with this hypothesis, Grem1$^+$PDGFRα$^+$ stromal cells expressing *Il1r1* (therefore, similar to YFP$^-$ cells) promote intestinal regeneration mediated by Rspo3 (Cox et al., 2021). The immature state of epithelial cells in LTBR$^{\Delta PDGFRa}$ mice, including decrease in goblet cells and tight junctions, as well as dysregulation of RA signaling might

lead to dysregulated repair and increased susceptibility to intestinal inflammation (Kim and Ho, 2010; Van der Sluis et al., 2006; Collins et al., 2011). The basement membrane, and in particular laminins, are dysregulated in inflammatory bowel diseases (Spenlé et al., 2012), suggesting that dysregulated stromal maturation overall impacts on inflammation through several mechanisms.

Finally, we show that the main ligand of PDGFRα, *Pdgfa*, is strongly produced by epithelial cells, suggesting that subepithelial PDGFRα$^+$ stromal cells integrate signals from the epithelium to promote anti-inflammatory responses and epithelial integrity, both of which are essential for development of the intestinal barrier. As the LTBR lineage is perivascular and coexpresses PDGFRβ, proximity and availability of several PDGF ligands including PDGF-AA, PDGF-BB, and PDGF-C within the subepithelial and perivascular space is most likely key for proper position and function. Overall, these data suggest a tight control of the LTBR lineage by several mechanisms to ensure a timed development in the first few weeks after birth, when the intestine undergoes rapid villus and vascular remodeling to fulfill nutrient requirement, in order to promote intestinal barrier maturation and postnatal growth.

Limitations of the study

This study relies on BAC-transgenic fluorescent reporters, which serve as surrogates to evaluate cell identity and function by lineage tracing analysis. Specifically, we use LTBR to trace discrete perivascular stromal progenitors in the intestine, as previous reports have shown that LTBR-expressing perivascular stromal cells have progenitor functions in other organs. Further experiments will be required to determine whether LTBR is involved in regulation of stemness and cell fate of PDFGRα$^+$ postnatal progenitors, opening the possibility of additional control of intestinal stromal regulation by lymphotoxin α1β2 producing leucocytes, such as B cells, activated T cells, NK, or DCs. Moreover, the specific niche signals involved in the development and regulation of functionally distinct stromal lineages are still to be discovered.

STAR★METHODS

Detailed methods are provided in the online version of this paper and include the following:

- KEY RESOURCES TABLE
- RESOURCE AVAILABILITY
  - Lead contact
  - Materials availability
  - Data and code availability
- EXPERIMENTAL MODEL AND SUBJECT DETAILS
  - Mice
  - Mice treatment
- METHOD DETAILS
  - Tissue preparation and immunostaining
  - Cell isolation and flow cytometry
  - RNA Isolation and qRT-PCR
  - RNA sequencing
  - Cell culture
- QUANTIFICATION AND STATISTICAL ANALYSIS

SUPPLEMENTAL INFORMATION

Supplemental information can be found online at https://doi.org/10.1016/j.stem.2022.04.005.

ACKNOWLEDGMENTS

We thank all members of the Stroma, Inflammation & Tissue Repair Unit, as well as members from Microenvironment & Immunity Unit, for discussions; the Mouse Genetics Engineering Platform, the Cytometry Platform, and the ICM Institute for excellent technical support; and Jeffrey Browning for the kind gift of LTβR-Ig. J.-M.J., I.S., and A.B. were funded by fellowships from Le Ministère de l'Enseignement Supérieur et de la Recherche and Fondation pour la Recherche Médicale (FRM). This work has received funding from the Institut Pasteur, INSERM and the European Union's Horizon 2020 research and innovation program (ERC Consolidator grant No. 648428) to L.P.

AUTHOR CONTRIBUTIONS

Conceptualization, methodology, and validation, J.-M.J. and L.P.; mice experiments and data analysis, I.S., S.E.D.C., A.L., P.D.N., G.N., J.-M.J., and L.P.; RNA-seq analysis, R.L., H.V., and E.K.; single-cells analysis from public data, A.B.; writing – original draft, J.-M.J. and L.P.; funding acquisition, L.P.; supervision, L.P.

DECLARATION OF INTERESTS

The authors declare no competing interests.

Received: July 6, 2021
Revised: January 18, 2022
Accepted: April 7, 2022
Published: May 5, 2022

SUPPORTING CITATIONS

The following references appear in the supplemental information: Garcia et al., 2009; Nigro et al., 2014.

REFERENCES

Agace, W.W., and Persson, E.K. (2012). How vitamin A metabolizing dendritic cells are generated in the gut mucosa. Trends Immunol. *33*, 42–48.

Al Nabhani, Z., and Eberl, G. (2020). Imprinting of the immune system by the microbiota early in life. Mucosal Immunol. *13*, 183–189.

Allen, J.E., and Sutherland, T.E. (2014). Host protective roles of type 2 immunity: parasite killing and tissue repair, flip sides of the same coin. Semin. Immunol. *26*, 329–340.

Aoki, R., Shoshkes-Carmel, M., Gao, N., Shin, S., May, C.L., Golson, M.L., Zahm, A.M., Ray, M., Wiser, C.L., Wright, C.V.E., and Kaestner, K.H. (2016). Foxl1-expressing mesenchymal cells constitute the intestinal stem cell niche. Cell. Mol. Gastroenterol. Hepatol. *2*, 175–188.

Bakdash, G., Vogelpoel, L.T., Van Capel, T.M., Kapsenberg, M.L., and De Jong, E.C. (2015). Retinoic acid primes human dendritic cells to induce gut-homing, IL-10-producing regulatory T cells. Mucosal Immunol. *8*, 265–278.

Barker, N., Van Es, J.H., Kuipers, J., Kujala, P., Van Den Born, M., Cozijnsen, M., Haegebarth, A., Korving, J., Begthel, H., Peters, P.J., and Clevers, H. (2007). Identification of stem cells in small intestine and colon by marker gene Lgr5. Nature *449*, 1003–1007.

Batts, L.E., Polk, D.B., Dubois, R.N., and Kulessa, H. (2006). Bmp signaling is required for intestinal growth and morphogenesis. Dev. Dyn. *235*, 1563–1570.

Bénézech, C., Mader, E., Desanti, G., Khan, M., Nakamura, K., White, A., Ware, C.F., Anderson, G., and Caamaño, J.H. (2012). Lymphotoxin-beta receptor signaling through NF-kappaB2-RelB pathway reprograms adipocyte precursors as lymph node stromal cells. Immunity *37*, 721–734.

Bénézech, C., White, A., Mader, E., Serre, K., Parnell, S., Pfeffer, K., Ware, C.F., Anderson, G., and Caamaño, J.H. (2010). Ontogeny of stromal organizer cells during lymph node development. J. Immunol. *184*, 4521–4530.

Bry, L., Falk, P., Huttner, K., Ouellette, A., Midtvedt, T., and Gordon, J.I. (1994). Paneth cell differentiation in the developing intestine of normal and transgenic mice. Proc. Natl. Acad. Sci. USA *91*, 10335–10339.

Chin, A.M., Hill, D.R., Aurora, M., and Spence, J.R. (2017). Morphogenesis and maturation of the embryonic and postnatal intestine. Semin. Cell Dev. Biol. *66*, 81–93.

Collins, C.B., Aherne, C.M., Kominsky, D., Mcnamee, E.N., Lebsack, M.D., Eltzschig, H., Jedlicka, P., and Rivera-Nieves, J. (2011). Retinoic acid attenuates ileitis by restoring the balance between T-helper 17 and T regulatory cells. Gastroenterology *141*, 1821–1831.

Coombes, J.L., Siddiqui, K.R.R., Arancibia-Cárcamo, C.V., Hall, J., Sun, C.-M., Belkaid, Y., and Powrie, F. (2007). A functionally specialized population of mucosal CD103+ DCs induces Foxp3+ regulatory T cells via a TGF-β- and retinoic acid–dependent mechanism. J. Exp. Med. *204*, 1757–1764.

Cox, C.B., Storm, E.E., Kapoor, V.N., Chavarria-Smith, J., Lin, D.L., Wang, L., Li, Y., Kljavin, N., Ota, N., Bainbridge, T.W., et al. (2021). IL-1R1-dependent signaling coordinates epithelial regeneration in response to intestinal damage. Sci. Immunol. *6*, eabe8856.

Degirmenci, B., Valenta, T., Dimitrieva, S., Hausmann, G., and Basler, K. (2018). GLI1-expressing mesenchymal cells form the essential Wnt-secreting niche for colon stem cells. Nature *558*, 449–453.

Di Carlo, S.E., and Peduto, L. (2018). The perivascular origin of pathological fibroblasts. J. Clin. Invest. *128*, 54–63.

Ewels, P., Magnusson, M., Lundin, S., and Käller, M. (2016). MultiQC: summarize analysis results for multiple tools and samples in a single report. Bioinformatics *32*, 3047–3048.

Fütterer, A., Mink, K., Luz, A., Kosco-Vilbois, M.H., and Pfeffer, K. (1998). The lymphotoxin b receptor controls organogenesis and affinity maturation in peripheral lymphoid tissues. Immunity *9*, 59–70.

Garcia, M.I., Ghiani, M., Lefort, A., Libert, F., Strollo, S., and Vassart, G. (2009). LGR5 deficiency deregulates Wnt signaling and leads to precocious Paneth cell differentiation in the fetal intestine. Dev. Biol. *331*, 58–67.

Gjorevski, N., Sachs, N., Manfrin, A., Giger, S., Bragina, M.E., Ordóñez-Morán, P., Clevers, H., and Lutolf, M.P. (2016). Designer matrices for intestinal stem cell and organoid culture. Nature *539*, 560–564.

Greicius, G., Kabiri, Z., Sigmundsson, K., Liang, C., Bunte, R., Singh, M.K., and Virshup, D.M. (2018). *PDGFRα*$^{+}$ pericryptal stromal cells are the critical source of Wnts and RSPO3 for murine intestinal stem cells *in vivo*. Proc. Natl. Acad. Sci. USA *115*, E3173–E3181.

Groulx, J.F., Gagné, D., Benoit, Y.D., Martel, D., Basora, N., and Beaulieu, J.F. (2011). Collagen VI is a basement membrane component that regulates epithelial cell-fibronectin interactions. Matrix Biol. *30*, 195–206.

Haber, A.L., Biton, M., Rogel, N., Herbst, R.H., Shekhar, K., Smillie, C., Burgin, G., Delorey, T.M., Howitt, M.R., Katz, Y., et al. (2017). A single-cell survey of the small intestinal epithelium. Nature *551*, 333–339.

Hadis, U., Wahl, B., Schulz, O., Hardtke-Wolenski, M., Schippers, A., Wagner, N., Müller, W., Sparwasser, T., Förster, R., and Pabst, O. (2011). Intestinal tolerance requires gut homing and expansion of FoxP3+ regulatory T cells in the lamina propria. Immunity *34*, 237–246.

Hageman, J.H., Heinz, M.C., Kretzschmar, K., Van Der Vaart, J., Clevers, H., and Snippert, H.J.G. (2020). Intestinal regeneration: regulation by the microenvironment. Dev. Cell *54*, 435–446.

Hoch, R.V., and Soriano, P. (2003). Roles of PDGF in animal development. Development *130*, 4769–4784.

Iwata, M., Hirakiyama, A., Eshima, Y., Kagechika, H., Kato, C., and Song, S.Y. (2004). Retinoic acid imprints gut-homing specificity on T cells. Immunity *21*, 527–538.

Jiang, D., Liang, J., and Noble, P.W. (2007). Hyaluronan in tissue injury and repair. Annu. Rev. Cell Dev. Biol. *23*, 435–461.

Karlsson, L., Lindahl, P., Heath, J.K., and Betsholtz, C. (2000). Abnormal gastrointestinal development in PDGF-A and PDGFR-(alpha) deficient mice implicates a novel mesenchymal structure with putative instructive properties in villus morphogenesis. Development *127*, 3457–3466.

Kim, Y.S., and Ho, S.B. (2010). Intestinal goblet cells and mucins in health and disease: recent insights and progress. Curr. Gastroenterol. Rep. *12*, 319–330.

Kim, I., Yilmaz, O.H., and Morrison, S.J. (2005). CD144 (VE-cadherin) is transiently expressed by fetal liver hematopoietic stem cells. Blood *106*, 903–905. https://doi.org/10.1182/blood-2004-12-4960.

Koh, S.J., Choi, Y., Kim, B.G., Lee, K.L., Kim, D.W., Kim, J.H., Kim, J.W., and Kim, J.S. (2016). Matricellular protein Periostin mediates intestinal inflammation through the activation of nuclear factor kappa B signaling. PLoS One *11*, e0149652.

Kosinski, C., Li, V.S.W., Chan, A.S.Y., Zhang, J., Ho, C., Tsui, W.Y., Chan, T.L., Mifflin, R.C., Powell, D.W., Yuen, S.T., et al. (2007). Gene expression patterns of human colon tops and basal crypts and BMP antagonists as intestinal stem cell niche factors. Proc. Natl. Acad. Sci. USA *104*, 15418–15423.

Kosinski, C., Stange, D.E., Xu, C., Chan, A.S., Ho, C., Yuen, S.T., Mifflin, R.C., Powell, D.W., Clevers, H., Leung, S.Y., and Chen, X. (2010). Indian hedgehog regulates intestinal stem cell fate through epithelial-mesenchymal interactions during development. Gastroenterology *139*, 893–903.

Köster, J., and Rahmann, S. (2012). Snakemake—a scalable bioinformatics workflow engine. Bioinformatics *28*, 2520–2522.

Krautler, N.J., Kana, V., Kranich, J., Tian, Y., Perera, D., Lemm, D., Schwarz, P., Armulik, A., Browning, J.L., Tallquist, M., et al. (2012). Follicular dendritic cells emerge from ubiquitous perivascular precursors. Cell *150*, 194–206.

Kuo, H.J., Maslen, C.L., Keene, D.R., and Glanville, R.W. (1997). Type VI collagen anchors endothelial basement membranes by interacting with type IV collagen. J. Biol. Chem. *272*, 26522–26529.

Laffont, S., Siddiqui, K.R., and Powrie, F. (2010). Intestinal inflammation abrogates the tolerogenic properties of MLN CD103+ dendritic cells. Eur. J. Immunol. *40*, 1877–1883.

Lantier, L., Lacroix-Lamandé, S., Potiron, L., Metton, C., Drouet, F., Guesdon, W., Gnahoui-David, A., Le Vern, Y., Deriaud, E., Fenis, A., et al. (2013). Intestinal CD103+ dendritic cells are key players in the innate immune control of Cryptosporidium parvum infection in neonatal mice. PLoS Pathog. *9*, e1003801.

Li, J., and Hoyle, G.W. (2001). Overexpression of PDGF-A in the lung epithelium of transgenic mice produces a lethal phenotype associated with hyperplasia of mesenchymal cells. Dev. Biol. *239*, 338–349.

Love, M.I., Huber, W., and Anders, S. (2014). Moderated estimation of fold change and dispersion for RNA-seq data with DESeq2. Genome Biol. *15*, 550.

Lu, T.T., and Browning, J.L. (2014). Role of the lymphotoxin/LIGHT system in the development and maintenance of reticular networks and vasculature in lymphoid tissues. Front. Immunol. *5*, 47.

Lukonin, I., Serra, D., Challet Meylan, L., Volkmann, K., Baaten, J., Zhao, R., Meeusen, S., Colman, K., Maurer, F., Stadler, M.B., et al. (2020). Phenotypic landscape of intestinal organoid regeneration. Nature *586*, 275–280.

Macho-Fernandez, E., Koroleva, E.P., Spencer, C.M., Tighe, M., Torrado, E., Cooper, A.M., Fu, Y.X., and Tumanov, A.V. (2015). Lymphotoxin beta receptor signaling limits mucosal damage through driving IL-23 production by epithelial cells. Mucosal Immunol. *8*, 403–413.

Mahapatro, M., Foersch, S., Hefele, M., He, G.W., Giner-Ventura, E., Mchedlidze, T., Kindermann, M., Vetrano, S., Danese, S., Günther, C., et al. (2016). Programming of intestinal epithelial differentiation by IL-33 derived from pericryptal fibroblasts in response to systemic infection. Cell Rep. *15*, 1743–1756.

Mccarthy, N., Manieri, E., Storm, E.E., Saadatpour, A., Luoma, A.M., Kapoor, V.N., Madha, S., Gaynor, L.T., Cox, C., Keerthivasan, S., et al. (2020). Distinct mesenchymal cell populations generate the essential intestinal BMP signaling gradient. Cell Stem Cell *26*, 391–402.e5.

Muncan, V., Heijmans, J., Krasinski, S.D., Büller, N.V., Wildenberg, M.E., Meisner, S., Radonjic, M., Stapleton, K.A., Lamers, W.H., Biemond, I., et al. (2011). Blimp1 regulates the transition of neonatal to adult intestinal epithelium. Nat. Commun. *2*, 452.

Ng, Y.L., Klopcic, B., Lloyd, F., Forrest, C., Greene, W., and Lawrance, I.C. (2013). Secreted protein acidic and rich in cysteine (SPARC) exacerbates colonic inflammatory symptoms in dextran sodium sulphate-induced murine colitis. PLoS One *8*, e77575.

Nigro, G., Rossi, R., Commere, P.H., Jay, P., and Sansonetti, P.J. (2014). The cytosolic bacterial peptidoglycan sensor Nod2 affords stem cell protection and links microbes to gut epithelial regeneration. Cell Host Microbe *15*, 792–798.

Noah, T.K., Donahue, B., and Shroyer, N.F. (2011). Intestinal development and differentiation. Exp. Cell Res. *317*, 2702–2710.

Oliveira, L.M., Teixeira, F.M.E., and Sato, M.N. (2018). Impact of retinoic acid on immune cells and inflammatory diseases. Mediators Inflamm. *2018*, 3067126.

Olson, L.E., and Soriano, P. (2009). Increased PDGFRα activation disrupts connective tissue development and drives systemic fibrosis. Dev. Cell *16*, 303–313.

Peduto, L., Dulauroy, S., Lochner, M., Späth, G.F., Morales, M.A., Cumano, A., and Eberl, G. (2009). Inflammation recapitulates the ontogeny of lymphoid stromal cells. J. Immunol. *182*, 5789–5799.

Perez-Shibayama, C., Gil-Cruz, C., and Ludewig, B. (2019). Fibroblastic reticular cells at the nexus of innate and adaptive immune responses. Immunol. Rev. *289*, 31–41.

Persson, E.K., Scott, C.L., Mowat, A.M., and Agace, W.W. (2013). Dendritic cell subsets in the intestinal lamina propria: ontogeny and function. Eur. J. Immunol. *43*, 3098–3107.

Powell, D.W., Pinchuk, I.V., Saada, J.I., Chen, X., and Mifflin, R.C. (2011). Mesenchymal cells of the intestinal lamina propria. Annu. Rev. Physiol. *73*, 213–237.

Qi, Z., Li, Y., Zhao, B., Xu, C., Liu, Y., Li, H., Zhang, B., Wang, X., Yang, X., Xie, W., et al. (2017). BMP restricts stemness of intestinal Lgr5+ stem cells by directly suppressing their signature genes. Nat. Commun. *8*, 13824.

Reinhardt, C., Bergentall, M., Greiner, T.U., Schaffner, F., Ostergren-Lundén, G., Petersen, L.C., Ruf, W., and Bäckhed, F. (2012). Tissue factor and PAR1 promote microbiota-induced intestinal vascular remodelling. Nature *483*, 627–631.

Rennert, P.D., James, D., Mackay, F., Browning, J.L., and Hochman., P.S. (1998). Lymph node genesis is induced by signaling through the lymphotoxin beta receptor. Immunity *9*, 71–79. https://doi.org/10.1016/s1074-7613(00)80589-0.

Ruane, D.T., and Lavelle, E.C. (2011). The role of CD103(+) dendritic cells in the intestinal mucosal immune system. Front. Immunol. *2*, 25.

Sartor, R.B. (1997). Review article: how relevant to human inflammatory bowel disease are current animal models of intestinal inflammation? Aliment. Pharmacol. Ther. *11*, 89–96. discussion 96–97.

Schirbel, A., Kessler, S., Rieder, F., West, G., Rebert, N., Asosingh, K., Mcdonald, C., and Fiocchi, C. (2013). Pro-angiogenic activity of TLRs and NLRs: a novel link between gut microbiota and intestinal angiogenesis. Gastroenterology *144*, 613–623.e9.

Schönig, K., Schwenk, F., Rajewsky, K., and Bujard, H. (2002). Stringent doxycycline dependent control of CRE recombinase *in vivo*. Nucleic Acids Res. *30*, e134.

Schuijers, J., Van Der Flier, L.G., Van Es, J., and Clevers, H. (2014). Robust cre-mediated recombination in small intestinal stem cells utilizing the olfm4 locus. Stem Cell Rep. *3*, 234–241.

Schulz, O., Jaensson, E., Persson, E.K., Liu, X., Worbs, T., Agace, W.W., and Pabst, O. (2009). Intestinal CD103+, but not CX3CR1+, antigen sampling cells migrate in lymph and serve classical dendritic cell functions. J. Exp. Med. *206*, 3101–3114.

Shoshkes-Carmel, M., Wang, Y.J., Wangensteen, K.J., Tóth, B., Kondo, A., Massasa, E.E., Itzkovitz, S., and Kaestner, K.H. (2018). Subepithelial telocytes are an important source of Wnts that supports intestinal crypts. Nature *557*, 242–246.

Sigthorsson, G., Simpson, R.J., Walley, M., Anthony, A., Foster, R., Hotz-Behoftsitz, C., Palizban, A., Pombo, J., Watts, J., Morham, S.G., and Bjarnason, I. (2002). COX-1 and 2, intestinal integrity, and pathogenesis of nonsteroidal anti-inflammatory drug enteropathy in mice. Gastroenterology *122*, 1913–1923.

Simon-Assmann, P., Lefebvre, O., Bellissent-Waydelich, A., Olsen, J., Orian-Rousseau, V., and De Arcangelis, A. (1998). The laminins: role in intestinal morphogenesis and differentiation. Ann. N. Y. Acad. Sci. *859*, 46–64.

Sparwasser, T., Gong, S., Li, J.Y.H., and Eberl, G. (2004). General method for the modification of different BAC types and the rapid generation of BAC transgenic mice. Genesis *38*, 39–50.

Spenlé, C., Hussenet, T., Lacroute, J., Lefebvre, O., Kedinger, M., Orend, G., and Simon-Assmann, P. (2012). Dysregulation of laminins in intestinal inflammation. Pathol. Biol. (Paris) *60*, 41–47.

Srinivas, S., Watanabe, T., Lin, C.S., William, C.M., Tanabe, Y., Jessell, T.M., and Costantini, F. (2001). Cre reporter strains produced by targeted insertion of EYFP and ECFP into the ROSA26 locus. BMC Dev. Biol. *1*, 4.

Stappenbeck, T.S., Hooper, L.V., and Gordon, J.I. (2002). Developmental regulation of intestinal angiogenesis by indigenous microbes via Paneth cells. Proc. Natl. Acad. Sci. USA *99*, 15451–15455.

Stzepourginski, I., Eberl, G., and Peduto, L. (2015). An optimized protocol for isolating lymphoid stromal cells from the intestinal lamina propria. J. Immunol. Methods *421*, 14–19.

Stzepourginski, I., Nigro, G., Jacob, J.M., Dulauroy, S., Sansonetti, P.J., Eberl, G., and Peduto, L. (2017). CD34+ mesenchymal cells are a major component of the intestinal stem cells niche at homeostasis and after injury. Proc. Natl. Acad. Sci. USA *114*, E506–E513.

Tanoue, T., Atarashi, K., and Honda, K. (2016). Development and maintenance of intestinal regulatory T cells. Nat. Rev. Immunol. *16*, 295–309.

Van Der Flier, L.G., and Clevers, H. (2009). Stem cells, self-renewal, and differentiation in the intestinal epithelium. Annu. Rev. Physiol. *71*, 241–260.

Van Der Flier, L.G., Van Gijn, M.E., Hatzis, P., Kujala, P., Haegebarth, A., Stange, D.E., Begthel, H., Van Den Born, M., Guryev, V., Oving, I., et al. (2009). Transcription factor achaete scute-like 2 controls intestinal stem cell fate. Cell *136*, 903–912.

Van Der Sluis, M., De Koning, B.A.E., De Bruijn, A.C.J.M., Velcich, A., Meijerink, J.P.P., Van Goudoever, J.B., Büller, H.A., Dekker, J., Van Seuningen, I., Renes, I.B., and Einerhand, A.W.C. (2006). Muc2-deficient mice spontaneously develop colitis, indicating that MUC2 is critical for colonic protection. Gastroenterology *131*, 117–129.

Varet, H., Brillet-Guéguen, L., Coppée, J.Y., and Dillies, M.A. (2016). SARTools: a DESeq2- and EdgeR-based R pipeline for comprehensive differential analysis of RNA-Seq data. PLoS One *11*, e0157022.

Vicente-Suarez, I., Larange, A., Reardon, C., Matho, M., Feau, S., Chodaczek, G., Park, Y., Obata, Y., Gold, R., Wang-Zhu, Y., et al. (2015). Unique lamina propria stromal cells imprint the functional phenotype of mucosal dendritic cells. Mucosal Immunol *8*, 141–151.

Zhuo, Y., Hoyle, G.W., Shan, B., Levy, D.R., and Lasky, J.A. (2006). Overexpression of PDGF-C using a lung specific promoter results in abnormal lung development. Transgen. Res. *15*, 543–555.

STAR★METHODS

KEY RESOURCES TABLE

REAGENT or RESOURCE	SOURCE	IDENTIFIER
Antibodies		
PE-conjugated anti-podoplanin (8.1.1)	BioLegend	Cat# 127407;RRID:AB_2161929
Syrian hamster anti-podoplanin (8.1.1)	Gift from J. Browning	N/A
BV786-conjugated anti-CD31 (390)	BD Biosciences	Cat# 740879; RRID:AB_2740529
APC-conjugated anti-CD31 (MEC.13.3)	BD Biosciences	Cat# 551262; RRID:AB_398497
Rabbit anti-GFP (polyclonal)	ThermoFischer	Cat# A-11122; RRID:AB_221569
PE-Texas-Red-conjugated anti-CD45 (30-F11)	BD Biosciences	Cat# 562420; RRID:AB_11154401
Biotinylated anti-PDGFRa (APA5)	ThermoFischer	Cat# 13-1401-82; RRID:AB_466607
Goat anti-PDGFRa (polyclonal)	R&D System	Cat# AF1062; RRID:AB_2236897
Rat anti-E-Cadherin (DECMA-1)	Abcam	Cat# Ab11512; RRID:AB_298118
Rabbit anti-Lysozyme1 (polyclonal)	ThermoFischer	Cat# PA5-16668; RRID:AB_10984852
Wheat Germ Agglutinin	ThermoFisher	Cat# ICN790162, RRID:AB_2334867
APC-conjugated anti-CD3 (145-2C11)	BioLegend	Cat# 100311; RRID:AB_312676
BV650-conjugated anti-CD19	BioLegend	Cat# 302238; RRID:AB_2562097
APC-eF780-conjugated anti-CD11c (N418)	ThermoFischer	Cat# 47-0114-82; RRID:AB_1548652
FITC-conjugated anti-MHC-II (M5/114.15.2)	ThermoFischer	Cat# 11-5321-82; RRID:AB_465232
BV785-conjugated anti-CD103 (M290)	BD Biosciences	Cat# 563087; RRID:AB_2721775
Pe-Cy7-conjugated anti-CD11b (M1/70)	BioLegend	Cat# 101216; RRID:AB_312799
BV421-conjugated anti-Siglec F	BD Biosciences	Cat# 562681; RRID:AB_2722581
BV605-conjugated anti-Ly6C	BD Biosciences	Cat# 563011; RRID:AB_2737949
PerCP-cy5.5-conjugated anti-Ly6G	BioLegend	Cat# 127616; RRID:AB_1877271
FITC-conjugated anti-CD4 (RM4-5)	BioLegend	Cat# 100510; RRID:AB_312713
PerCP-Cy5.5-conjugated anti-Foxp3 (FJK-16s)	ThermoFischer	Cat# 45-5773-82; RRID:AB_914351
PerCP-Cy5.5-conjugated anti-Isotype IgG2a,k (eBR2a)	ThermoFischer	Cat# 45-4321-80; RRID:AB_906259
Pe-conjugated anti-Lymphotoxin beta Receptor (eBio3C8)	ThermoFischer	Cat# 12-5671-82, RRID:AB_2016713
Chemicals, peptides, and recombinant proteins		
Ampicillin	Sigma-Aldrich	Cat# A9518
Dextran sulfate 40 sodium salt BioChemic	PanReacAppliChem	Cat# A3261
EDTA 0.5M, pH 8.0	Invitrogen	Cat# AM9262
Metronidazole	Sigma-Aldrich	Cat# M3761
Streptomycin	Sigma-Aldrich	Cat# S6501
Vancomycin	Sigma-Aldrich	Cat# V1150
Amphotericin B	Sigma-Aldrich	Cat# A4888
DAPI	Sigma-Aldrich	Cat# 10236276001
Recombinant Murine Flt3-Ligand	Preprotech	Cat# 250-31L
Recombinant Murine GM-CSF	Preprotech	Cat# 315-03
Murine PDGF-AA	Preprotech	Cat# 315-17
Indomethacin	Sigma-Aldrich	Cat# I7378
Doxycycline hyclate	Sigma-Aldrich	Cat# D9891
Critical commercial assays		
Fixable Blue Dead Cell Stain Kit	Invitrogen	Cat# L23105
Fixation-permeabilization buffer	eBioscience	Cat# 00-5521-00

(*Continued on next page*)

Continued

REAGENT or RESOURCE	SOURCE	IDENTIFIER
Aldefluor Kit	StemCell Technologies	Cat# 01700
Click-iT™ EdU Cell Proliferation Kit for Imaging, AF™ 647 dye	ThermoFischer	Cat# C10340
Single Cell RNA Purification Kit	Norgen	Cat# 51800
Qubit RNA HS kit	ThermoFischer	Cat# Q32852
Qubit dsDNA HS kit	ThermoFischer	Cat# Q32854
Agilent RNA 6000 Pico Kit	Agilent	Cat# 5067-1513
SuperScript IV Reverse Transcriptase	Invitrogen	Cat# 18090010
SsoAdvanced Universal SYBR Green Supermix	BioRad	Cat# 1725275
SMARTer® Stranded Total RNA-SeqKit v2-Pico Input	Takara Bio	Cat# 634412
NextSeq 500/550 High Output Kit v2.5 (75 Cycles)	Illumina	Cat# 20024906
Deposited data		
Raw and processed RNAseq data of intestinal YFP^{+} and YFP^{-} stromal cells	This paper	GEO: GSE200362
Raw and processed RNAseq data of intestinal YFP^{+} and YFP^{-} stromal cells after indomethacin	This paper	GEO: GSE200364
Raw and processed RNAseq data of intestinal YFP^{+}PDGFRα^{+} and YFP^{+}PDGFRα^{-} stromal cells	This paper	GEO: GSE200363
Experimental models: Organisms/strains		
Ltbr-Cre-IRES-eGFP	This paper	N/A
Ltbr-tTA-IRES-DTR	This paper	N/A
Pdgfra^{floxed} (Pdgfra-tm8Sor/EiJ)	The Jackson Laboratory	JAX stock #006492
LC1 (Tg(tetO-cre)LC1Bjd)	Schonig et al., 2002	MGI:2448952
Rosa26^{EYFP} (B6.129X1-*Gt(ROSA)26Sor$^{tm1(EYFP)Cos}$*/J)	Srinivas et al., 2001	JAX stock #006148
Lgr5-eGFP-IRES-CreERT2 (B6.129P2-*Lgr5$^{tm1(cre/ERT2)Cle}$*/J)	The Jackson Laboratory	JAX stock #008875
VE-Cadherin-Cre (B6.FVB-Tg(Cdh5-cre) 7Mlia/J)	The Jackson Laboratory	JAX stock #006137
Oligonucleotides		
qRT-PCR mouse Axin2 primer assay	Biorad	qMmuCED0044828
qRT-PCR mouse Muc2 primer assay	Biorad	qMmuCID0019583
qRT-PCR mouse Tff3 primer assay	Biorad	qMmuCID0008757
qRT-PCR mouse Tjp2 primer assay	Biorad	qMmuCEP0054545
qRT-PCR mouse Sis primer assay	Biorad	qMmuCID0015908
qRT-PCR mouse Il18 primer assay	Biorad	qMmuCID0005876
qRT-PCR mouse Il1b primer assay	Biorad	qMmuCID0005641
qRT-PCR mouse Pdgfa primer assay	Biorad	qMmuCID0022342
qRT-PCR mouse Cdk1 primer assay	Biorad	qMmuCID0015611
qRT-PCR mouse Mki67 primer assay	Biorad	qMmuCED0047197
Additional primers are found in Table S1	N/A	N/A
Software and algorithms		
R project for Statistical Computing	R foundation	RRID: SCR_001905
DESeq2	Love et al., 2014	Bioconductor DESeq2
FlowJo-v10	FlowJo, LLC	RRID:SCR_008520
Prism 6	GraphPad	RRID: SCR_002798

(*Continued on next page*)

Continued

REAGENT or RESOURCE	SOURCE	IDENTIFIER
ZEN Image Acquisition Software	Zeiss Microscope	RRID: SCR_013672
Fiji	Image J	RRID: SCR_002285
Adobe Photoshop CC	Adobe Systems	RRID: SCR_014199
Other		
RNAscope probe: Mm-*Lgr5*	ACDBio	312171

RESOURCE AVAILABILITY

Lead contact

Further information and requests for resources and reagents should be directed to and will be fulfilled by the lead contact, Lucie Peduto (lucie.peduto@pasteur.fr).

Materials availability

Material generated in this study is available from the lead contact upon request, with a completed Materials Transfer Agreement.

Data and code availability

- The raw data of bulk RNA-seq generated by this study have been deposited in NCBI's Gene Expression Omnibus and are accessible through GEO Series accession number GEO: GSE200365. Accession numbers of each dataset are listed in the key resources table.
- This paper does not report original code.
- Any additional information required to reanalyze the data reported in this work paper is available from the lead contact upon request.

EXPERIMENTAL MODEL AND SUBJECT DETAILS

Mice

All mice were kept in specific pathogen-free conditions, and mouse experiments were approved by the committee on animal experimentation of the Institut Pasteur and by the French Ministry of Agriculture. Co-housed non-transgenic littermates were used as controls in all experiments; experimental groups were both age and sex matched. All mice were C57BL/6 background. We generated BAC-transgenic *LTBR-cre-ires-egfp* mice ($LTBR^{GFP}$), by inserting the coding sequence for *cre-ires-egfp*, including a poly(A) sequence after *egfp*, into exon 1 of *Ltbr* in place of the endogenous ATG translation start codon, on a 200-kb BAC (Invitrogen) carrying 80 kb of sequence upstream of the *Ltbr* translation start site. The transgene insertion was done by homologous recombination as described (Sparwasser et al., 2004). We generated BAC-transgenic *Ltbr-tTA-ires-Dtr* mice ($LTBR^{tTA}$), by inserting the coding sequence for *tTA-ires-Dtr* (human), including a poly(A) sequence after *Dtr*, into exon 1 of *Ltbr* in place of the endogenous ATG translation start codon, on a 200-kb BAC as described above. We carried out inducible fate mapping experiments in triple-transgenic $LTBR^{YFP}$ mice obtained by crossing $LTBR^{tTA}$ mice with tet-inducible LC1 mice (Schonig, 2002), and with $Rosa26^{floxSTOP\text{-}YFP}$ mice (Srinivas et al., 2001). In both BAC-transgenic models, GFP and YFP expression was consistent with reported expression of LTβR. Inducible conditional ablation of PDGFRα in the LTBR lineage was achieved by crossing $LTBR^{tTA}$ mice to tet-regulated Cre (LC1) mice and $PDGFR\alpha^{fl/fl}$ mice (Jackson Laboratories) to obtain $LTBR^{\triangle PDGFRa}$ mice. In some experiments, $LTBR^{\triangle PDGFRa}$ mice were further crossed to $Rosa26^{floxSTOP\text{-}YFP}$ mice ($LTBR^{\triangle PDGFRa/YFP}$ mice). Lgr5-EGFP-IRES-creERT2 mice (Barker et al., 2007) were purchased from The Jackson Laboratories. VE-cadherin-*Cre* mice specifically express *Cre* by vascular endothelial-cadherin (Cdh5) (The Jackson Laboratories) were crossed to $Rosa26^{floxSTOP\text{-}YFP}$ mice for lineage tracing studies.

Mice treatment

To stop gene labeling or gene excision in the tTA mice models, doxycycline (Sigma-Aldrich) at 1 mg/ml was added in drinking water containing 5% sucrose, during the indicated periods of time. To assess epithelial proliferation, mice were injected i.p. with 80μl of EdU 10mM and analyzed 2 hours after injection. To induce intestinal ulcers, mice were injected intra-peritoneally with indomethacin (10mg/kg). To visualize ulcers, mice were injected with Evan's Blue 1% intra-venously 30 min before killing. Intestines were opened, pinned down and intestinal ulcers were counted and their area was measured using Fiji based on evan's blue diffusion. To induce intestinal inflammation, mice were treated with Dextran Sodium Sulfate (DSS) 2,5% in drinking water for one week. To deplete the microbiota, mice were treated from late gestation with 2.5 mg/ml streptomycin, 1 mg/ml ampicillin, 0.5 mg/ml vancomycin, metronidazole 0.5 mg/ml and amphotericin b 0.1mg/mL in the drinking water. The antibiotic-containing drinking water was changed twice a week.

METHOD DETAILS

Tissue preparation and immunostaining

Intestines were washed, opened and fixed overnight at 4°C in solution of 4% paraformaldehyde (PFA). For immunofluorescence, samples were washed for 24h in PBS, incubated for 2–4h in a solution of 30% sucrose in PBS, embedded in OCT, and frozen in a bath of isopentane cooled with liquid nitrogen. Frozen blocs were cut at 8um thickness and sections collected onto Superfrost Plus slides. Sections were processed for immunofluorescence staining: after 1h blocking with 10% bovine serum in PBS containing 0,1% Triton at room temperature, slides were incubated with primary antibodies at the appropriate concentration in PBS containing 1% bovine serum and 0,1% Triton (PBS-TS) overnight at 4°C, washed three times for 5 min with PBS-TS, incubated for 1h at room temperature with secondary antibodies or streptavidin at the appropriate concentration, washed once, incubated with DAPI (1ug/mL) for 5 min, washed three times for 5 min and mounted with Fluoromount-G (Southern Biotechnology Associates). For pathological assessment, intestines were fixed in PFA, incubated in ethanol and embedded in paraffin. Paraffin blocs were cut a 4μm for hematoxylin and eosin coloration. Lgr5 expression was detected with an RNAscope ISH assay (Advanced Cell Diagnostics - ACDBio), following the manufacturer's instructions. We examined slides with an AxioImager M1 fluorescence microscope (Zeiss) equipped with a CCD camera and processed images with AxioVision Zen software (Zeiss) or ImageJ software. The graphical abstract was created using Biorender.com.

Cell isolation and flow cytometry

To isolate cells from the small intestine lamina propria, Peyer's patches were removed, intestine opened longitudinally, cut into pieces and processed as we previously described (Stzepourginski et al., 2015). To isolate cells from the LN, LN were incubated for 30min in DMEM containing Liberase DL (1 Wunit/mL; Roche) and DNAse I (1 U/ml; ThermoFisher). Cells were filtered through a 100-um mesh in DMEM 10% BS, washed, filtered through a 40um filter in PBS 2% BS, and processed for FACS staining (Stzepourginski et al., 2015). Cells were incubated for 1 min with DAPI (Sigma) before analysis to exclude dead cells. When indicated, the fusion protein LTβR-Ig or IgG control proteins (Rennert et al., 1998) were pre-incubated with anti-LTβR antibodies. For intracellular FACS staining, we incubated cells with LIVE/DEADTM Fixable Blue Dead Cell Stain Kit following the manufacturer instruction, and processed for intracellular staining using FoxP3/Transcription Factor Staining Buffer Kit. Cells were fixed and permeabilized according to the manufacturer's instructions. Retinoic Acid production by dendritic cells was assessed using the Aldefluor kit according to manufacturer's instructions. Cell doublets were excluded during analysis. Cells were analyzed with Fortessa (BD Biosciences) and Flowjo software (Tristar) and isolated with FacsARIA III (BD Biosciences). The immune populations were gated as follow: $CD19^+$ cells were gated on $CD45^+$ cells, Th2 and Th17 were gated on $CD45^+CD3^+CD4^+$ cells, $CD8^+$ T cells were gated on $CD45^+CD3^+$ cells, ILC2 and ILC3 were gated on $CD45^+CD19^-CD3^-IL\text{-}7R^+$ cells, $CD103^+CD11b^-$ DCs and CX_3CR1^+ mononuclear phagocytes were gated on $CD45^+CD19^-CD3^-CD11c^{high}MHC\text{-}II^{high}$ cells, $SiglecF^+$ eosinophils, $Ly6G^{high}$ neutrophils and $Ly6C^{high}$ monocytes were gated on $CD45^+CD19^-CD3^-CD11c^{-/low}MHC\text{-}II^{-/low}CD11b^+$ cells.

RNA Isolation and qRT-PCR

We FACS sorted cells, or collected epithelial cells directly into vials containing lysis buffer complemented with 1% ß-mercaptoethanol. We isolated total RNA using the Single Cell RNA Purification Kit (Norgen) according to the manufacturer's instructions. We assessed the quality of total RNA using the 2100 Bioanalyzer system (Agilent Technologies) and the quantity using Qbit RNA HS kit (ThermoFischer). Total RNA was transcribed into cDNAs using SuperScript IV reverse transcriptase (Invitrogen). We performed qRT-PCR using RT^2-qPCR primer sets (Bio-Rad Laboratories) and SYBR-Green master mix (Bio-Rad Laboratories), on a PTC-200 thermocycler equipped with a Chromo4 detector (Bio-Rad Laboratories), and analyzed data using Opticon Monitor software (Bio-Rad Laboratories). Ct values were normalized to the mean of Ct values obtained for the housekeeping genes *Hsp90ab1, Hprt,* and *Gapdh*.

RNA sequencing

Librairies were prepared from total mRNA using the SMARTer® Stranded Total RNA-Seq Kit v2-Pico Input Mammalian (Takara Bio) according to the manufacturer's instruction. Library quality and quantity were assessed using the 2100 Bioanalyzer system (Agilent Technologies) and the Qbit dsDNA HS kit (ThermoFischer). Sequencing was performed using Illumina NextSeq 500/550 High Output kit v2.5. The RNA-seq analysis was performed with Sequana 0.11.0 (https://github.com/sequana/sequana_rnaseq) built on top of Snakemake 6.1.1 (Koster and Rahmann, 2012). Briefly, reads were trimmed from adapters using cutadapt 3.4 then mapped to the genome assembly GRCm38 from Ensembl using STAR 2.7.3a. FeatureCounts 2.0.1 was used to produce the count matrix, assigning reads to features using corresponding annotation GRCm38_92 from Ensembl with strand-specificity information. Quality control statistics were summarized using MultiQC 1.10.1 (Ewels et al., 2016). Clustering of transcriptomic profiles were assessed using a Principal Component Analysis (PCA). Differential expression testing was conducted using DESeq2 library 1.24.0 (Love et al., 2014) and SARTOOLS scripts (Varet et al., 2016). The normalization and dispersion estimation were performed with DESeq2 using the default parameters; statistical tests for differential expression were performed applying the independent filtering algorithm. A generalized linear model was set in order to test for the differential expression between conditions. Raw p-values were adjusted for multiple testing according to the Benjamini and Hochberg procedure and genes with an adjusted p-value lower than 0.05 were considered differentially expressed. Gene set enrichment analysis was performed using the fisher statistical test for the over-representation of up-regulated genes.

Cell culture

FACS sorted intestinal PDGFRα^{+}Pdpn^{+} stromal cells were plated in complete RPMI medium for 3 days. *In vitro* differentiation of CD103^{+}CD11b^{+} BM-DCs was performed as previously described. Briefly, one million total BM cells were cultured in CM containing GM-CSF (Preprotech, 20ng/mL) and FLT3L (Preprotech, 100ng/mL) with partial change of medium at day 3 and 5. At days 7, cells were collected. For experiments, DCs were co-cultured +/- stromal cells in complete medium lacking GM-CSF and FLT3L for 3 days, and analyzed by FACS. In some experiments, PDGFRα^{+}Pdpn^{+} stromal cells were incubated O/N with 20ng/mL of PDGF-AA in medium containing reduced serum.

QUANTIFICATION AND STATISTICAL ANALYSIS

For quantification of immunofluorescence stainings, we examined slides with an AxioImager M1 fluorescence microscope (Zeiss) equipped with a CCD camera. Images were processed with AxioVision Zen software (Zeiss) and quantified using ImageJ software on the indicated number of images per mice. Except for the RNAseq experiments, statistical significance between groups was determined using either Student's t tests, one or two-tailed as appropriate, using GraphPad Prism 6 (GraphPad Software, La Jolla, California). Unless otherwise specified, n represents the number of animals. Values are expressed as means ± standard deviation (SD). A p value < 0.05 was considered statistically significant. For all figures, asterisks denote statistical significance and the associated p values are shown in the legends.